This is the author's version of an article that has been published in this journal. Changes were made to this version by the publisher prior to publication.
The final version of record is available at http://dx.doi.org/10.1109/TCOMM.2020.2987565

Lattice-based Robust Distributed Source Coding for Three Correlated Sources

Sorina Dumitrescu, *Senior Member, IEEE*, Dania Elzouki, and Jun Chen, *Senior Member, IEEE*

***Abstract*—The problem of robust distributed source coding for three correlated sources is studied in this work. A lattice-based scheme is proposed and the analysis of its performance is provided in the high resolution regime. Special attention is paid to the degenerate case where the three sources are Gaussian and identical. In this case, our scheme is shown to achieve within an asymptotic gap of 0.069 bits in terms of rate per description from the information-theoretic limit of quadratic symmetric Gaussian multiple description coding with central and individual decoders, when the side distortion and the ratio between the central and side distortions both approach 0.**

***Index Terms*—Correlated sources, distributed source coding, lattice quantization, asymptotic performance analysis, high resolution, multiple description coding.**

I. Introduction

In distributed source coding (DSC), two or more correlated sources are encoded separately and transmitted to a common decoder. The fundamental information-theoretical limits are characterized in [1] for the lossless case, and in [2] for the lossy case assuming that all sources but one are directly available at the decoder. The general version of the lossy DSC problem was first treated by Berger [3] and Tung [4]. However, in spite of significant efforts over the past few decades, the conclusive solution has been determined only for certain particular cases [5]–[10]. An important variant of the DSC problem is known as the CEO (short for Chief Executive Officer) problem [11]. Oohama [12] and Prabhakaran *et al.* [13] have characterized completely the rate-distortion region for the CEO problem in the quadratic Gaussian case.

In the robust DSC (RDSC) problem, the channels connecting some of the encoders with the fusion center may break down. The robust version was addressed in the CEO scenario by Ishwar *et al.* [14] and Chen and Berger [15]. The development of practical schemes for RDSC was tackled in [16]–[18], but only locally optimal solutions were proposed.

In this work, we present a structured lattice-based coding scheme for the RDSC problem in the case of three correlated sources with a central decoder and three individual decoders (Figure 1). Note that lattices have been used in the previous works on the DSC problem [19]–[22]. A key technique employed in lossy DSC problems is quantization followed by binning. For this, Zamir *et al.* [19] proposed the use of *nested lattice codes*, i.e., a pair of nested lattices, where the fine lattice is utilized for quantization and the coarse lattice for binning. This idea was largely adopted by the other works as well. In addition, Krithivasan and Pradhan [21] considered the variant of the lossy DSC problem where a linear function of K Gaussian correlated sources is to be reconstructed at the decoder. They use nested lattice codes with *correlated binning*, i.e., where the different sources may use different fine lattices, but the coarse lattice has to be common. Most of the aforementioned works resort to dithered lattice quantization and analyze the system performance as the dimension of the lattices approaches ∞. One exception is the work of Servetto [20], which addresses the design of lattice-based schemes for the Wyner-Ziv problem[1] and performs the analysis as the rate approaches ∞ and the correlation between sources approaches 1.

The particular case of the RDSC problem where all sources are identical is known as the multiple description (MD) problem [23]–[31]. Lattices have been very popular in the design of MD schemes [32]–[41], [41]–[43]. Most of the aforementioned schemes ([32], [33], [35], [36], [38], [40]–[42]), referred to as MDLVQs (short for MD lattice vector quantizers), also rely on a pair of nested lattices and use as the key mechanism the *index assignment*, which is an injective mapping from the fine lattice to L-tuples of points from the coarse lattice, where L is the number of desired descriptions. More specifically, the source sequence is first quantized to the closest lattice point λ_c in the fine lattice. This quantizer is referred to as the *central quantizer* and the fine lattice is called the *central lattice*. The output of the central quantizer further undergoes the index assignment, generating the L-tuple $(\alpha_1(\lambda_c), \cdots, \alpha_L(\lambda_c))$ of points in the coarse lattice. For each $1 \le l \le L$, $\alpha_l(\lambda_c)$ represents the lth description and is used for reconstruction at the lth side decoder. The central decoder is able to recover λ_c and outputs it as the reconstruction. In these works, the asymptotic performance as the rate approaches ∞, for fixed lattice dimension is analyzed.

To the best of our knowledge, the lattice-based design for the RDSC problem was only addressed in our previous work [44] for the case of two correlated sources. The performance analysis of the scheme is derived for fixed lattice dimension n in a high resolution regime. For the case where the two sources are identical (which corresponds to the MD framework), the analysis reveals that the proposed scheme can achieve the information-theoretic limit of quadratic symmetric MD coding, when the side distortion and the ratio between the central and side distortions both go to 0, while $n \to \infty$. In [44], a variant of the random coding scheme that Chen and Berger

Sorina Dumitrescu and Jun Chen are with the Department of Electrical and Computer Engineering, McMaster University, Hamilton, Canada. Dania Elzouki was with the Department of Electrical and Computer Engineering, McMaster University, Hamilton, Canada. (Emails: sorina@mail.ece.mcmaster.ca elzoukda@mcmaster.ca; junchen@mail.ece.mcmaster.ca). This work was supported in part by two NSERC Discovery Grants.

[1]The Wyner-Ziv problem refers to the lossy source coding problem with side information available only at the decoder.

This is the author's version of an article that has been published in this journal. Changes were made to this version by the publisher prior to publication.
The final version of record is available at http://dx.doi.org/10.1109/TCOMM.2020.2987565

[15] proposed for the robust CEO problem was considered for comparison and it was proved that the sum-rate of the Chen-Berger scheme with Gaussian codes is 0.5 bits larger than the sum-rate of the lattice-based coding scheme in the same asymptotic regime.

The scheme in [44] employs three nested lattices $\Lambda_s \subset \Lambda_{in} \subset \Lambda_c$. For $i = 1, 2$, encoder i quantizes the source sequence to the closest point $\lambda_{c,i}$ in Λ_c, and $\lambda_{c,i}$ is further quantized to the closest point λ_i in Λ_{in}. Next, a mapping $\beta_i : \Lambda_{in} \to \Lambda_s$ is applied and $\beta_i(\lambda_i)$ is sent to the decoder. The point $\beta_i(\lambda_i)$ in the coarsest lattice will be used for reconstruction at the side decoder i. Encoder i also transmits some additional information, via Slepian-Wolf coding[2], to be used at the central decoder to jointly refine the reconstructions of the two source sequences. Part of this supplementary information is $\lambda_{c,i} - \lambda_i$, which can be interpreted as a bin index. Thus, the lattice Λ_{in} can be regarded as the counterpart of the coarse lattice used for binning in the previous works on lattice-based lossy DSC. It should be noted that in the aforementioned works, the decoder is able to recover the finely quantized points with high probability as the dimension n of the lattice approaches ∞. Since [44] is concerned with fixed lattice dimension, some more information is transmitted to enhance the performance at the central decoder. A novel idea introduced in [44] is to use the knowledge about the closeness of the input sequences to infer at each encoder some information about the other sequence. Specifically, each encoder operates under the assumption that the two sequences are within some distance r_0. Then, if $\lambda_{c,i}$ is too close to the boundary of the Voronoi region of the lattice Λ_{in}, encoder i concludes that the other sequence could be in a different Voronoi region and sends some supplementary information to help at the central decoder. In this way, when the input sequences are indeed within the distance r_0 from each other, the central decoder will output $\lambda_{c,1}$ and $\lambda_{c,2}$ as reconstructions. Otherwise, the reconstructions will have essentially the same quality as at the side decoders. Thus, the probability that the input sequences are not within the distance r_0 influences the system performance.

The mappings β_i proposed in [44] are inspired by the concept of index assignment employed in MDLVQ. However, the requirements that the mappings β_i need to satisfy are more difficult to meet in the scenario of non-identical sources. For this reason and in order to facilitate the analysis of system performance, linear mappings are used.

In this work we propose a lattice-based scheme for the RDSC problem in the case of three correlated sources. The proposed scheme can be regarded as an extension of the framework of [44], but it is not a trivial one. One major challenge when transitioning from two to three sources is the design of mappings $\beta_i, i = 1, 2, 3$. To make the relevant analysis tractable, it is important to ensure the linearity of these mappings. This turns out to be much more complicated than in the case of two sources because the constraints the mappings need to satisfy are more complex. We tackle this design problem[3] by introducing an additional lattice Λ_f such that $\Lambda_s \subset \Lambda_f \subset \Lambda_{in}$. Moreover, the fact that the mappings β_i are more complex than in the case of two sources is a reason for added complexity at the encoder and at the central decoder. Specifically, there are more situations where the encoders need to transmit additional information for the purpose of helping the central decoder make the correct decision. This also leads to more cases to be addressed at the central decoder. It is worth emphasizing that, because of this additional complexity some aspects in the proofs of the theoretical results have to be handled differently than in [44]. We provide the performance analysis of the proposed scheme under the high resolution assumption. In the degenerate case where the three sources are identical and Gaussian, our scheme is compared with the MDLVQ of [35] in the asymptotic regime where both the side distortion and the ratio between the central and side distortions approach 0. The asymptotic analysis shows that our scheme has only a small rate loss of 0.069 bits per description in comparison with the MDLVQ of [35], when $n \to \infty$. In view of the fact (pointed out in [41]) that the MDLVQ of [35] achieves the information-theoretical limit of the quadratic symmetric Gaussian MDC problem with individual and central decoders (derived in [25]) in the aforementioned asymptotic regime as $n \to \infty$, we conclude that our scheme can achieve within an asymptotic gap of 0.069 bits[4] from the fundamental limit in terms of rate per description.

Finally, we point out that [45] is a shortened conference version of this work, which does not include the proofs of the theoretical results.

The rest of this paper is divided into five sections. In Section II, the notations and definitions used throughout this work are introduced. Section III presents the main result, i.e., the asymptotic analysis of the performance of the proposed RDSC scheme. In Section IV, the comparison with the MDLVQ scheme of [35] is performed when the three sources are identical and Gaussian. Section V presents in detail the operation of the proposed scheme. Lastly, Section VI concludes the paper.

II. Definitions and Notation

Consider three sources (X_1, X_2, X_3) with joint probability density function (pdf) $f_{X_1 X_2 X_3}$. They generate a jointly i.i.d. random process $(X_{1i}, X_{2i}, X_{3i})_{i \in \mathbb{N}}$. The marginal density function of each X_j will be denoted by f_{X_j}, $j = 1, 2, 3$. We aim to construct a robust distributed source coding system as depicted in Figure 1. The system is comprised of three encoders and four decoders. Encoder i has source X_i as its input, $i = 1, 2, 3$. Side decoder i receives the message transmitted by encoder i, $i = 1, 2, 3$. The central decoder receives the messages from all three encoders. The squared error is used as the distortion measure.

The following definitions will be used throughout the work. Let Y be a discrete random variable with values in the alphabet $\mathcal{Y}$ and with probability mass function p_Y. If $\sum_{y \in \mathcal{Y}} p_Y(y) \log_2 p_Y(y)$ is finite, then the entropy of Y is defined as $H(Y) \triangleq -\sum_{y \in \mathcal{Y}} p_Y(y) \log_2 p_Y(y)$. If $X^n \in \mathbb{R}^n$

[2]Slepian-Wolf coding refers to optimal distributed lossless compression of correlated sources.

[3]See Remark 3 for more insights regarding our design.

[4]A possible explanation for this gap is provided in Remark 4.

This is the author's version of an article that has been published in this journal. Changes were made to this version by the publisher prior to publication.
The final version of record is available at http://dx.doi.org/10.1109/TCOMM.2020.2987565

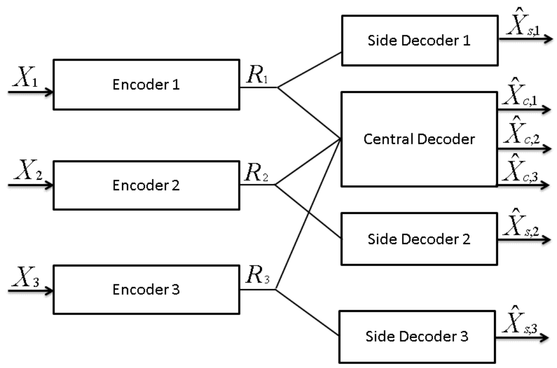

Fig. 1. Robust distributed source coding for three correlated sources.

is a continuous random vector with pdf f_{X^n}, and the quantity $\int_{\mathbb{R}^n} f_{X^n}(x^n)\log_2 f_{X^n}(x^n)dx^n$ is finite, then the differential entropy of X^n is $h(X^n) \triangleq -\int_{\mathbb{R}^n} f_{X^n}(x^n)\log_2 f_{X^n}(x^n)dx^n$.

We will use the notation $\|x^n\|$ for the Euclidian norm of the row vector $x^n \in \mathbb{R}^n$. $\mathbf{0}$ denotes the all-zero vector in $\mathbb{R}^n$. For any set $\mathcal{A} \subseteq \mathbb{R}^n$, any $a \in \mathbb{R}$, and any $x^n \in \mathbb{R}^n$, let $x^n + \mathcal{A} \triangleq \{x^n + y^n | y^n \in \mathcal{A}\}$ and $a\mathcal{A} \triangleq \{ay^n | y^n \in \mathcal{A}\}$. For any measurable set $\mathcal{A} \subseteq \mathbb{R}^n$, let $\nu(\mathcal{A})$ denote its volume, i.e., $\nu(\mathcal{A}) \triangleq \int_{\mathcal{A}} dx^n$. Further, let $\mathcal{B}_r \triangleq \{x^n \in \mathbb{R}^n | \|x^n\| < r\}$.

An n-dimensional lattice $\Lambda \subset \mathbb{R}^n$ is defined as follows

$$\Lambda \triangleq \{\lambda \in \mathbb{R}^n | \lambda = z^n \cdot \mathbf{G}, z^n \in \mathbb{Z}^n\},$$

where $\mathbf{G}$ is a non-singular n-by-n matrix with elements in $\mathbb{R}$. Each lattice Λ has an associated quantizer $Q_\Lambda(\cdot)$ which maps each $x^n \in \mathbb{R}^n$ to its closest lattice point, i.e.,

$$Q_\Lambda(x^n) \triangleq \arg\min_{\lambda \in \Lambda} \|x^n - \lambda\|. \tag{1}$$

For each $\lambda \in \Lambda$, the set of all points which are assigned by Q_Λ to λ forms the *Voronoi cell (or region)* $V_\Lambda(\lambda)$ *of* λ *in* Λ. The ties in (1) are broken in a systematic manner so that the following holds

$$V_\Lambda(\lambda) = \lambda + V_\Lambda(\mathbf{0}),\ \forall \lambda \in \Lambda.$$

For any $\mathcal{A} \subseteq \mathbb{R}^n$, let $\overline{\mathcal{A}}$ be the closure of $\mathcal{A}$, i.e., the union of $\mathcal{A}$ and its boundary. Then one has

$$\overline{V_\Lambda(\lambda)} = \{x^n \in \mathbb{R}^n | \|x^n - \lambda\| \leq \|x^n - \lambda'\| \text{ for every } \lambda' \in \Lambda\}.$$

It is important to emphasize that, in view of our definition of the Voronoi region, which agrees with [46], not every point on the boundary of $V_\Lambda(\lambda)$ belongs to $V_\Lambda(\lambda)$, therefore $\overline{V_\Lambda(\lambda)} \neq V_\Lambda(\lambda)$. Two disjoint subsets of $\mathbb{R}^n$ are said to be *adjacent* if the intersection of their closures is not empty. Additionally, define for any $x^n \in \mathbb{R}^n$,

$$x^n \bmod \Lambda \triangleq x^n - Q_\Lambda(x^n).$$

A *fundamental cell of the lattice* Λ is a bounded set $\mathcal{C}_0$ such that the sets $\lambda + \mathcal{C}_0$, for all $\lambda \in \Lambda$, form a partition of $\mathbb{R}^n$. We will denote by ν_Λ the volume of a fundamental cell of the lattice Λ. Notice that $\nu_\Lambda = \nu(V_\Lambda(\mathbf{0}))$.

An important notion related to quantization is the *normalized second moment* of a measurable set $\mathcal{A} \subseteq \mathbb{R}^n$, which is defined as

$$G(\mathcal{A}) \triangleq \frac{\int_{\mathcal{A}} \|x^n\|^2 dx^n}{n\nu(\mathcal{A})^{\frac{2}{n}+1}}.$$

It is obvious that the normalized second moment is not changed under the scaling operation. We will use the notation G_Λ for the *normalized second moment of the lattice* Λ, which is defined as

$$G_\Lambda \triangleq G(V_\Lambda(\mathbf{0})).$$

For any set $\mathcal{A} \subset \mathbb{R}^n$, denote $\bar{r}(\mathcal{A}) \triangleq \sup_{x^n \in \mathcal{A}} \|x^n\|$. The value $\bar{r}_\Lambda \triangleq \bar{r}(V_\Lambda(\mathbf{0}))$ is called the *covering radius* of the lattice Λ. The *inscribed radius* of the lattice Λ, denoted by r_Λ, is the radius of the largest open ball centered in $\mathbf{0}$ and included in $V_\Lambda(\mathbf{0})$.

Lattices (Λ_1, Λ_2) are called *nested* if $\Lambda_2 \subset \Lambda_1$, which means that Λ_2 is a sublattice of Λ_1. The term *fine lattice* is used for Λ_1, while Λ_2 is referred to as the *coarse lattice*. The index of Λ_2 with respect to Λ_1 is $N(\Lambda_2 : \Lambda_1) \triangleq \frac{\nu_{\Lambda_2}}{\nu_{\Lambda_1}}$.

For any $\lambda_1 \in \Lambda_1$, the set $\lambda_1 + \Lambda_2$ is said to be a *coset of* Λ_2 *relative to* Λ_1. A set $\mathcal{F} \subset \Lambda_1$ is called a *set of coset representatives of* Λ_2 *relative to* Λ_1 if the following equalities are satisfied

$$\Lambda_1 = \cup_{\lambda_1 \in \mathcal{F}} (\lambda_1 + \Lambda_2),\ (\lambda_1 + \Lambda_2) \cap (\lambda_1' + \Lambda_2) = \emptyset$$
$$\text{for all } \lambda_1 \neq \lambda_1' \in \mathcal{F}.$$

From the above relations it follows that every point $\lambda \in \Lambda_1$ can be expressed in a unique manner as $\lambda = \lambda_1 + \lambda_2$ where $\lambda_1 \in \mathcal{F}$ and $\lambda_2 \in \Lambda_2$. As proved in [46], if $\mathcal{C}_0$ is a fundamental cell of Λ_2, then $\mathcal{C}_0 \cap \Lambda_1$ is a set of coset representatives of Λ_2 relative to Λ_1. Furthermore, we denote $V_{\Lambda_2:\Lambda_1} \triangleq V_{\Lambda_2}(\mathbf{0}) \cap \Lambda_1$ and $\mathcal{C}_{\Lambda_2:\Lambda_1} \triangleq \cup_{\lambda_1 \in V_{\Lambda_2:\Lambda_1}} V_{\Lambda_1}(\lambda_1)$.

Given a quantizer Q on $\mathbb{R}^n$ and a random vector $X^n \in \mathbb{R}^n$, let $D(Q, X^n)$ denote the expected distortion per sample, i.e., $D(Q, X^n) \triangleq \frac{1}{n}\mathbb{E}\left[\| Q(X^n) - X^n \|^2\right]$.

III. Main Results

As we have already mentioned, the main contribution of this work is the design of a lattice-based RDSC scheme for the case of three correlated sources. This section presents the main results regarding the performance analysis of the proposed scheme, while the detailed description of the scheme will be treated in Section V.

In the sequel, we assume that each of the three sources has a continuous and bounded pdf with finite variance and differential entropy. Without loss of generality we also assume that each marginal pdf has mean 0.

A *lattice robust distributed source code* (LRDSC) of dimension n is specified by a positive value r_0 and four n-dimensional nested lattices $\Lambda_s \subset \Lambda_f \subset \Lambda_{in} \subset \Lambda_c \subset \mathbb{R}^n$. We will denote the LRDSC as $\mathcal{L}^{(n,r_0)} = (\Lambda_s, \Lambda_f, \Lambda_{in}, \Lambda_c)$. The *central* lattice Λ_c will be used at the central decoder for the reconstruction of each source, while the *side* lattice Λ_s is used to reconstruct the sources at the side decoders. The lattices

Λ_{in} and Λ_f are auxiliary lattices used in the operation of the scheme. The *intermediate* lattice Λ_{in} is constructed such that the following condition

$$r_0 + 2\bar{r}_c \leq r_{in} \tag{2}$$

is satisfied, where r_{in} is the inscribed radius of Λ_{in}, and $\bar{r}_c$ is the covering radius of Λ_c. The lattice Λ_f is defined as $\Lambda_f = c_0\Lambda_{in}$, while $\Lambda_s = 3c_0\Lambda_f$, where c_0 is a positive integer. It follows that $\Lambda_s = 3c_0^2\Lambda_{in}$. The lattice $\Lambda_{s/3} \triangleq \frac{1}{3}\Lambda_s$ is called the *fractional* lattice. It is utilized during the operation of the proposed scheme. Notice that $\Lambda_s \subset \Lambda_{s/3} \subset \Lambda_f$.

For $i = 1, 2, 3$, encoder i maps the source sequence x_i^n to the nearest point $\lambda_{c,i}$ in the central lattice, which is further mapped to the nearest point λ_i in Λ_{in}. A mapping $\beta_i : \Lambda_{in} \to \Lambda_s$ is next applied and $\beta_i(\lambda_i)$ is transmitted. $\beta_i(\lambda_i)$ will be used as reconstruction at the side decoder i. In addition, encoder i transmits some supplementary information to be used at the central decoder to refine the reconstruction. The LRDSC scheme is designed such that, when the input sequences x_1^n, x_2^n, x_3^n are at distance at most r_0 from each other, the central decoder is able to output the central lattice points $\lambda_{c,1}, \lambda_{c,2}, \lambda_{c,3}$ as reconstructions of the three sources, respectively. If the aforementioned condition is violated, i.e., at least two of the input sequences are at a distance larger than r_0, the quality of the reconstruction achieved at the central decoder is essentially the same as at the corresponding side decoder. Therefore, the following quantity plays an important role in the analysis of the performance of the proposed scheme

$$\mathcal{P}_{X_1X_2X_3}(r_0) \triangleq \mathbb{P}[X_1^n - X_2^n \notin \mathcal{B}_{r_0} \text{ or } X_2^n - X_3^n \notin \mathcal{B}_{r_0} \text{ or } X_1^n - X_3^n \notin \mathcal{B}_{r_0}]. \tag{3}$$

As it will be apparent shortly, the value r_0 controls the trade-off between the rate at the encoders and the fidelity of the reconstruction obtained at the central decoder.

In order to assess the performance of the LRDSC $\mathcal{L}^{(n,r_0)}$, we assume that m sequences x_i^n are input into each encoder i, one at a time. The corresponding m outputs will be further compressed losslessly. The rates and distortions of the LRDSC $\mathcal{L}^{(n,r_0)}$ are defined in the limit of m going to ∞. The rate of encoder i, $i = 1, 2, 3$, is denoted by $R_i(\mathcal{L}^{(n,r_0)})$. For each $i = 1, 2, 3$, the reconstruction distortion of source X_i at the side decoder i, referred to as side distortion, is denoted by $d_{s,i}(\mathcal{L}^{(n,r_0)})$, while the reconstruction distortion at the central decoder is $d_{c,i}(\mathcal{L}^{(n,r_0)})$ and is referred to as central distortion. Finally, we denote $d_s(\mathcal{L}^{(n,r_0)}) \triangleq \frac{\sum_{i=1}^{3} d_{s,i}(\mathcal{L}^{(n,r_0)})}{3}$.

For simplifying the lattice-related notation, we will utilize in the rest of the manuscript only the subscripts c, in, f, $s/3$, s, instead of Λ_c, Λ_{in}, Λ_f, $\Lambda_{s/3}$, Λ_s, respectively. For instance, we will use ν_s instead of ν_{Λ_s}. Let $K \triangleq N(\Lambda_{in} : \Lambda_c) = \frac{\nu_{in}}{\nu_c}$ and $M \triangleq N(\Lambda_s : \Lambda_{in}) = \frac{\nu_s}{\nu_{in}}$. Since $\Lambda_s = 3c_0^2\Lambda_{in}$, it follows that $M = 3^n c_0^{2n}$.

The performance of the proposed lattice-based scheme is evaluated for fixed dimension n and fixed K, as ν_c, ν_{in} and ν_s approach 0, while $M \to \infty$ and $\sqrt{M}\nu_s \to 0$. Thus, we will consider some fixed lattices $\Lambda_{c,0}$ and $\Lambda_{in,0}$ and the scale factors θ and c_0 such that

$$\Lambda_c = \theta\Lambda_{c,0}, \quad \Lambda_{in} = \theta\Lambda_{in,0}, \tag{4}$$
$$\Lambda_s = 3c_0^2\theta\Lambda_{in,0}, \quad \Lambda_f = c_0\theta\Lambda_{in,0}. \tag{5}$$

The asymptotic regime we consider in this work is defined by the following relations

$$\theta \to 0, \quad c_0 \to \infty, \quad c_0^3\theta \to 0. \tag{6}$$

The following theorem, whose proof is deferred to Appendix B, evaluates the distortions and rates for the proposed scheme, in the limit of (6).

Theorem 1. *Let (X_1, X_2, X_3) be a fixed triple of correlated sources such that each pdf f_{X_i}, $i = 1, 2, 3$, is continuous and bounded with finite variance and differential entropy. Additionally, consider a fixed integer $n > 0$ and a family of LRDSCs $\mathcal{L}^{(n,r_0)} = (\Lambda_s, \Lambda_f, \Lambda_{in}, \Lambda_c)$ satisfying (4), (5) and (6). For $i = 1, 2, 3$, let $U_i \triangleq Q_c(X_i^n) \bmod \Lambda_{in}$. Then in the asymptotic regime specified by (6),*

$$d_s(\mathcal{L}^{(n,r_0)}) = \frac{4}{9} G_s M^{\frac{1}{n}} \nu_s^{\frac{2}{n}} (1 + o(1)), \tag{7}$$
$$G_c\nu_c^{\frac{2}{n}}(1 + o(1)) \leq d_{c,i}(\mathcal{L}^{(n,r_0)}) \leq \frac{1}{3n}\mathcal{P}_{X_1X_2X_3}(r_0)\kappa_1^2 M^{\frac{1}{n}}\nu_s^{\frac{2}{n}} + G_c\nu_c^{\frac{2}{n}}(1 + o(1)),\ i = 1, 2, 3, \tag{8}$$
$$R_i(\mathcal{L}^{(n,r_0)}) = h(X_i) - \frac{1}{n}\log_2(\nu_s) + \frac{1}{3n}H(U_1, U_2, U_3) + o(1),\ i = 1, 2, 3, \tag{9}$$

where κ_1 is a positive constant. Additionally, in each of relations (7)-(9), the term hidden in the little-o notation can be upperbounded by a function which approaches 0 under (6) and does not depend on the joint pdf $f_{X_1X_2X_3}$.

Remark 1. *We would like to point out that the condition that the marginal pdfs be bounded is needed only for the proof of relations (9). It is also important to note that this condition is only mildly restrictive since the pdfs which are relevant in practice are likely to fulfill it. For instance, any continuous pdf f_X satisfying $\lim_{|x|\to\infty} f_X(x) = 0$ is necessarily bounded.*

Clearly, Theorem 1 implies that when $\mathcal{P}_{X_1X_2X_3}(r_0)$ is sufficiently small, the central distortion is dominated by $G_c\nu_c^{\frac{2}{n}}$. This result is stated next.

Corollary 1. *Let f_X be a continuous and bounded pdf with finite variance and differential entropy. Additionally, consider a fixed integer $n > 0$, and a family of LRDSCs $\mathcal{L}^{(n,r_0)} = (\Lambda_s, \Lambda_f, \Lambda_{in}, \Lambda_c)$ satisfying (4), (5) and (6). Each LRDSC is applied to a triple of correlated sources (X_1, X_2, X_3) with marginal pdfs equal to f_X, satisfying the inequality*

$$\mathcal{P}_{X_1X_2X_3}(r_0) \leq \frac{\epsilon}{M^{\frac{3}{n}}},$$

where $\lim_{(6)} \epsilon = 0$. It follows that, in the limit of (6),

$$d_{c,i}(\mathcal{L}^{(n,r_0)}) = G_c\nu_c^{\frac{2}{n}}(1 + o(1)),\ i = 1, 2, 3,$$

where the term hidden in the little-o notation can be upper-bounded by a function which approaches 0 under (6) and depends on the joint pdf $f_{X_1X_2X_3}$ only through $\mathcal{P}_{X_1X_2X_3}(r_0)$.

IV. Comparison with MDLVQ

In this section we consider the case when all three sources are identical and Gaussian, which corresponds to the multiple description scenario. We compare the performance of the proposed coding scheme at high resolution with that of the MDLVQ of [35]. We will use the performance analysis of the MDLVQ of [35] derived in [41]. Note that the authors of [41] also proved that the MDLVQ of [35] approaches the fundamental limit of the quadratic symmetric Gaussian multiple description problem when only the reconstructions based on individual descriptions and all descriptions are of interest (derived in [25]) at high resolution, as the vector dimension approaches infinity.

Note that the limits (6) are equivalent to $d_s \to 0$ and $\frac{d_c}{d_s} \to 0$, where $d_c = d_{c,1} = d_{c,2} = d_{c,3}$ and $d_s = \frac{d_{s,1}+d_{s,2}+d_{s,3}}{3}$. Clearly, $U_1 = U_2 = U_3$ since we assume all three sources are identical. Then relations (9) become

$$\lim_{d_s \to 0, \frac{d_c}{d_s} \to 0} \left(R_i - h(X_i) + \frac{1}{n} \log_2 \nu_s - \frac{1}{3n} H(U_i) \right) = 0, \quad (10)$$

where we use R_i instead of $R_i(\mathcal{L}^{(n,r_0)})$.

It can be shown as in [44] that $\lim\limits_{(6)} H(U_i) = \log_2 K$, for $i = 1, 2, 3$. Plugging in (10), we obtain that

$$\lim_{d_s \to 0, \frac{d_c}{d_s} \to 0} \left(R_i - h(X_i) + \frac{1}{n} \log_2 \nu_s - \frac{1}{3n} \log_2 K \right) = 0, \quad (11)$$

for $i = 1, 2, 3$. Consider now an n-dimensional MDLVQ as in [35]. Let R_{MD} denote the rate of each description and let $d_{s,MD}$ denote the side distortion. For comparison we will assume that the central lattice used in the MDLVQ is the same lattice Λ_c as in our scheme. This implies that $d_{c,MD} = d_c$. Additionally, we also assume that $d_{s,MD} = d_s$. Let S_n denote the n-dimensional ball of radius 1, let $\tilde{\nu_s}$ be the volume of the Voronoi region of the side lattice used in the MDLVQ, and let $\tilde{K} = \frac{\tilde{\nu_s}}{\nu_c}$. According to [41], when $d_s \to 0$ and $\frac{d_c}{d_s} \to 0$, one has

$$d_{s,MD} = \frac{2}{3^{\frac{3}{2}}} \tilde{K}^{\frac{3}{n}} G(S_{2n}) \nu_c^{\frac{2}{n}} (1 + o(1)), \quad (12)$$

$$\lim_{d_s \to 0, \frac{d_c}{d_s} \to 0} \left(R_{MD} - h(X_1) + \frac{1}{n} \log_2 \tilde{\nu_s} \right) = 0. \quad (13)$$

Using the latter relation, together with $K = \frac{\nu_{in}}{\nu_c}$, (11) and (13), one obtains

$$\lim_{d_s \to 0, \frac{d_c}{d_s} \to 0} (R_{MD} - R_i) = \frac{1}{3n} \lim_{d_s \to 0, \frac{d_c}{d_s} \to 0} \log_2 \left(\left(\frac{\nu_s}{\tilde{\nu_s}} \right)^3 \frac{\nu_c}{\nu_{in}} \right). \quad (14)$$

Using (7), (12), $M = \frac{\nu_s}{\nu_{in}}$ and $\tilde{K} = \frac{\tilde{\nu_s}}{\nu_c}$ leads to

$$\frac{d_s}{d_{s,MD}} = \frac{2G_s}{\sqrt{3} G(S_{2n})} \left(\left(\frac{\nu_s}{\tilde{\nu_s}} \right)^3 \frac{\nu_c}{\nu_{in}} \right)^{\frac{1}{n}} \frac{1 + o(1)}{1 + o(1)}.$$

Letting $d_{s,MD} = d_s$ further yields

$$\lim_{d_s \to 0, \frac{d_c}{d_s} \to 0} \left(\left(\frac{\nu_s}{\tilde{\nu_s}} \right)^3 \frac{\nu_c}{\nu_{in}} \right)^{\frac{1}{n}} = \frac{\sqrt{3} G(S_{2n})}{2G_s}.$$

The above relation, combined with (14), implies that

$$\lim_{d_s \to 0, \frac{d_c}{d_s} \to 0} (R_{MD} - R_i) = \frac{1}{3} \log_2 \left(\frac{\sqrt{3} G(S_{2n})}{2G_s} \right). \quad (15)$$

It was shown in [47] that there is a sequence of lattices Λ_n such that $\lim_{n\to\infty} G(\Lambda_n) = \frac{1}{2\pi e} = \lim_{n\to\infty} G(S_{2n})$. Based on this result and (15), it follows that, for $i = 1, 2, 3$,

$$\lim_{n \to \infty} \lim_{d_s \to 0, \frac{d_c}{d_s} \to 0} (R_{MD} - R_i) = \frac{1}{3} \log_2 \frac{\sqrt{3}}{2} \approx -0.0692. \quad (16)$$

Remark 2. *A possible reason for the gap in (16) is discussed in Remark 4 in the following section. Interestingly, the value achieved in (15) for $n = 1$ is -0.0914, which is already very close to the asymptotical value reached when $n \to \infty$. However, the absolute value of the quantity in (15) is not a decreasing function of n as can be seen from Table I.*

TABLE I
The gap in (15) for several values of n. For each n, the lattice Λ_s is the optimal n-dimensional lattice for quantization reported in [48].

n	$\frac{1}{3} \log_2 \left(\frac{\sqrt{3} G(S_{2n})}{2G_s} \right)$
1	-0.0914
2	-0.1012
3	-0.1090
4	-0.1094
5	-0.1126
6	-0.1110
7	-0.1095
8	-0.1048
12	≈ -0.1074
16	≈ -0.1030
24	≈ -0.0944

V. Description of the Proposed LRDSC Scheme

In this section, we provide a detailed description of the LRDSC scheme.

A. Preliminaries

The following lemma, made possible by condition (2), is crucial for the subsequent development. Its proof is similar to the proof of Lemma 1 in [44] and therefore it is omitted.

Lemma 1. *For $i, j \in \{1, 2, 3\}$, if $x_j^n - x_i^n \in \mathcal{B}_{r_0}$, then*

$$\|Q_c(x_j^n) - Q_c(x_i^n)\| < r_{in},$$
$$\|Q_{in}(Q_c(x_j^n)) - Q_{in}(Q_c(x_i^n))\| < 3\bar{r}_{in}.$$

Further, we will define three labeling functions $\beta_i : \Lambda_{in} \to \Lambda_s$, for $i = 1, 2, 3$. Specifically, for any $\lambda \in \Lambda_{in}$, define

$$\beta_1(\lambda) \triangleq 3c_0 \tilde{\lambda_f} + \lambda_s, \quad \beta_2(\lambda) \triangleq 3c_0^2 \tilde{u_f} + \lambda_s,$$
$$\beta_3(\lambda) \triangleq 3\tau - 3c_0 \tilde{\lambda_f} - 3c_0^2 \tilde{u_f} + \lambda_s, \quad (17)$$

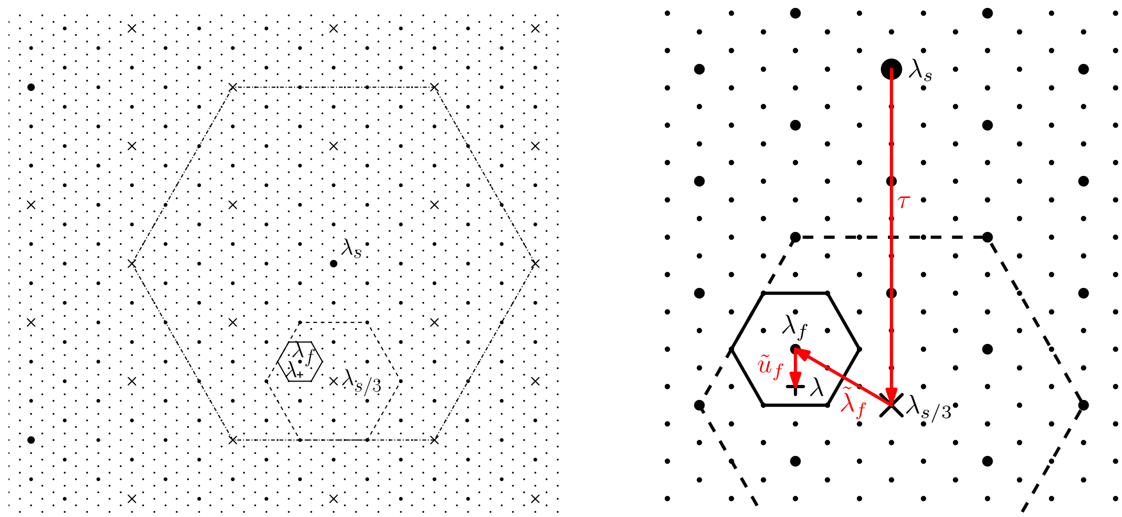

(a) (b)

Fig. 2. a) Illustration of the lattices $\Lambda_s, \Lambda_{s/3}, \lambda_f$ and Λ_{in}. The value of c_0 is 3. The small dots, the medium dots and the big dots are points in Λ_{in}, Λ_f, and Λ_s, respectively. The crosses are points in $\Lambda_{s/3} \setminus \Lambda_s$. The point λ, marked with a plus sign, is in Λ_{in}. The points λ_f, $\lambda_{s/3}$ and λ_s satisfy $\lambda_f = Q_f(\lambda)$, $\lambda_{s/3} = Q_{s/3}(\lambda_f)$ and $\lambda_s = Q_s(\lambda_{s/3})$. The small hexagon is the boundary of $V_f(\lambda_f)$. The big hexagon is the boundary of $V_s(\lambda_s)$. The middle-sized hexagon is the boundary of $V_{s/3}(\lambda_{s/3})$. b) Magnified portion illustrating the vectors $\tilde{u}_f = \lambda - \lambda_f$, $\tilde{\lambda}_f = \lambda_f - \lambda_{s/3}$ and $\tau = \lambda_{s/3} - \lambda_s$.

where

$$\tilde{u_f} \triangleq \lambda \bmod \Lambda_f = \lambda - Q_f(\lambda),$$
$$\tilde{\lambda_f} \triangleq Q_f(\lambda) \bmod \Lambda_{s/3} = Q_f(\lambda) - Q_{s/3}(Q_f(\lambda)),$$
$$\tau \triangleq Q_{s/3}(Q_f(\lambda)) \bmod \Lambda_s = Q_{s/3}(Q_f(\lambda)) - Q_s(Q_{s/3}(Q_f(\lambda))),$$
$$\lambda_s \triangleq Q_s(Q_{s/3}(Q_f(\lambda))).$$

Figures 2(a) and 2(b) illustrate a point λ along with $Q_f(\lambda)$, $Q_{s/3}(Q_f(\lambda))$, $Q_s(Q_{s/3}(Q_f(\lambda)))$, $\tilde{u}_f$, $\tilde{\lambda}_f$ and τ.

Note that the above definitions of $\tilde{u_f}, \tilde{\lambda_f}, \tau$ and λ_s imply that $\tilde{u}_f \in V_{\Lambda_f:\Lambda_{in}}$, $\tilde{\lambda}_f \in V_{\Lambda_{s/3}:\Lambda_f}$, $\tau \in V_{\Lambda_s:\Lambda_{s/3}}$, $\lambda_s \in \Lambda_s$ and

$$\lambda = \tilde{u}_f + \tilde{\lambda}_f + \tau + \lambda_s. \tag{18}$$

In the sequel we will consider the following simplified notation: $\mathcal{T} \triangleq V_{\Lambda_s:\Lambda_{s/3}}$, $\mathcal{L} \triangleq V_{\Lambda_{s/3}:\Lambda_f}$ and $\mathcal{F} \triangleq V_{\Lambda_f:\Lambda_{in}}$. Then $|\mathcal{T}| = N(\Lambda_s : \Lambda_{s/3}) = 3^n$, $|\mathcal{L}| = N(\Lambda_{s/3} : \Lambda_f) = c_0^n$ and $|\mathcal{F}| = N(\Lambda_f : \Lambda_{in}) = c_0^n$. Further, denote

$$\mathcal{U} \triangleq \{\tau + \tilde{\lambda}_f + \tilde{u}_f | \tau \in \mathcal{T}, \tilde{u}_f \in \mathcal{F}, \tilde{\lambda}_f \in \mathcal{L}\}. \tag{19}$$

Then $\mathcal{U}$ is a set of coset representatives of Λ_s relative to Λ_{in}. It follows that $|\mathcal{U}| = N(\Lambda_s : \Lambda_{in}) = M$ and

$$\Lambda_{in} = \bigcup_{\lambda \in \mathcal{U}} (\lambda + \Lambda_s).$$

The definition of the mappings β_i implies that they obey the *shift-invariance property*, i.e.,

$$\beta_i(\lambda + \tilde{\lambda}_s) = \beta_i(\lambda) + \tilde{\lambda}_s, \ \forall \lambda \in \Lambda_{in}, \ \forall \tilde{\lambda}_s \in \Lambda_s, \ i = 1, 2, 3. \tag{20}$$

Based on the shift-invariance property the following equalities are obtained, for $i = 1, 2, 3$, [44, Eq. (40), (41)],

$$\beta_i^{-1}(\lambda_s) = \beta_i^{-1}(\mathbf{0}) + \lambda_s, \forall \lambda_s \in \Lambda_s, \tag{21}$$
$$\beta_i^{-1}(\mathbf{0}) = \{\lambda - \beta_i(\lambda) | \lambda \in \mathcal{U}\}. \tag{22}$$

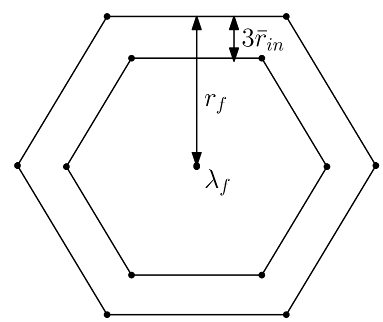

Fig. 3. The set $\mathcal{W}(\lambda_f)$ is the region between the two hexagons in the figure.

Remark 3. *The design of the mappings $\beta_i, i = 1, 2, 3$, was partly inspired by the index assignment used in the MDLVQ literature. More specifically, we borrowed from the work on MDLVQ the requirement that the mappings be shift-invariant, which boils down to defining $\beta_i(\lambda)$ as the sum of λ_s and a function of $\lambda - \lambda_s$. The second aspect inspired from the prior work on MDLVQ is the condition*

$$\beta_1(\lambda) + \beta_2(\lambda) + \beta_3(\lambda) = Q_{s/3}(Q_f(\lambda)), \tag{23}$$

which is adapted from the requirement imposed in [35] that $\alpha_1(\lambda) + \alpha_2(\lambda) + \alpha_3(\lambda) = Q_{s/3}(\lambda)$. On the other hand, unlike the MDLVQ literature, we also impose the linearity condition for the following reasons: 1) to make it easier to verify that the finest lattice points $\lambda_{c,1}, \lambda_{c,2}, \lambda_{c,3}$ can be recovered at the central decoder; 2) to simplify the performance analysis. A pleasant byproduct of the linearity is that structured decoding rules can be used, as we will see in the next subsection.

Note that linear mappings were also used in [44] for the case of two sources, but it was not straightforward to extend the construction of [44] to three sources, while ensuring that the central decoder recovers the finest lattice points when the input sequences are within the distance r_0 from one another.

We decided to introduce the additional lattice Λ_f, which enables the decomposition (18). Having this decomposition, our choices for β_1 and β_2 seemed natural, while β_3 was determined based on (23).

Remark 4. *The proof of relation (7) reveals that while $d_{s,1}$ and $d_{s,2}$ are roughly equal, $d_{s,3}$ is about twice larger. If $d_{s,3}$ could be brought down to the value of $d_{s,1}$, then the constant $\frac{4}{9}G_s$ in equation (7) would be replaced by $\frac{3}{9}G_s$, which would lead to the disappearance of the gap in (16). The reason why $d_{s,3}$ is twice larger than $d_{s,1}$ is that the variables $\tilde{\lambda}_f$ and $\tilde{u}_f$ used to define the mappings β_i are independent, thus the magnitude of $3c_0\tilde{\lambda}_f + 3c_0^2\tilde{u}_f$ essentially equals the sum of the magnitudes of the two terms, which implies that $\|\beta_1(\lambda)+\beta_2(\lambda)\| \approx \|\beta_1(\lambda)\| + \|\beta_2(\lambda)\|$, for $\lambda \in \mathcal{U}$. Thus, to avoid the gap in (16), while maintaining the condition (23), $\beta_1(\lambda)$ and $\beta_2(\lambda)$ have to be defined such that $\|\beta_1(\lambda)+\beta_2(\lambda)\| \approx \|\beta_1(\lambda)\| \approx \|\beta_2(\lambda)\|$, for $\lambda \in \mathcal{U}$. One possible solution is to let $\beta_2(\lambda)-\lambda_{s/3}$ be a fixed suitable transformation of $\beta_1(\lambda)-\lambda_{s/3}$, where $\lambda_{s/3} = Q_{s/3}(Q_f(\lambda))$. However, it remains to be established if such a definition can guarantee the recovery at the central decoder of the finest lattice points $\lambda_{c,1}, \lambda_{c,2}, \lambda_{c,3}$ when the input sequences are within the distance r_0 from one another. This line of inquiry will be pursued in future work.*

B. LRDSC Operation

The following discussion highlights the rationale underlying the proposed scheme. Let us denote $\lambda_i = Q_{in}(Q_c(x_i^n))$, for $i = 1,2,3$. The proposed scheme is developed in such a way that side decoder i is able to reconstruct $\beta_i(\lambda_i)$, and the central decoder reconstructs $\lambda_{c,i} = Q_c(x_i^n)$, for $i = 1,2,3$, when the source sequences are close enough in Euclidian distance, i.e., $x_j^n - x_i^n \in \mathcal{B}_{r_0}$ for all $i,j \in \{1,2,3\}$. Nevertheless, for the central decoder to reach this objective some supplementary information has to be conveyed in addition to $\beta_1(\lambda_1)$, $\beta_2(\lambda_2)$ and $\beta_3(\lambda_3)$. The amount of this supplementary information is decreased when λ_1, λ_2 and λ_3 are all in the same Voronoi region of Λ_f. Encoder i cannot identify all the situations when this happens since it only knows the sequence x_i^n, but not the other two source sequences. However, in view of Lemma 1, if $\lambda_i \in V_f(\lambda_f)$ and the distance from λ_i to the boundary of $V_f(\lambda_f)$ is not smaller than $3\bar{r}_{in}$, then encoder i concludes that the other sequences are also in $V_f(\lambda_f)$ when $x_j^n - x_i^n \in \mathcal{B}_{r_0}$ for all $i,j \in \{1,2,3\}$. Thus, we define the set

$$\begin{aligned}&\mathcal{W} \triangleq \cup_{\lambda_f\in\Lambda_f}\mathcal{W}(\lambda_f), \text{ where}\\ &\mathcal{W}(\lambda_f) \triangleq V_f(\lambda_f) \setminus (\lambda_f + \eta V_f(\mathbf{0})),\end{aligned} \tag{24}$$

for $\eta \triangleq 1 - \frac{3\bar{r}_{in}}{r_f}$ as shown in Figure 3. According to Lemma 1, if $\lambda_i \notin \mathcal{W}$, then $\lambda_j, j \in \{1,2,3\}\setminus\{i\}$ belongs to the same Voronoi region of Λ_f as λ_i, i.e., $Q_f(\lambda_i) = Q_f(\lambda_j)$, when $x_i^n - x_j^n \in \mathcal{B}_{r_0}$.

On the other hand, when $Q_f(\lambda_i) \neq Q_f(\lambda_j)$, it is important to determine if $Q_f(\lambda_i)$ and $Q_f(\lambda_j)$ are in the same Voronoi cell of $\Lambda_{s/3}$ or not. Let us define, for $\lambda_{s/3} \in \Lambda_{s/3}$,

$$\tilde{V}_{s/3}(\lambda_{s/3}) \triangleq \cup_{\lambda_f\in V_{s/3}(\lambda_{s/3})\cap\Lambda_f} V_f(\lambda_f). \tag{25}$$

The above definition implies that a point $\lambda \in \Lambda_{in}$ has $Q_{s/3}(Q_f(\lambda)) = \lambda_{s/3}$ if and only if $\lambda \in \tilde{V}_{s/3}(\lambda_{s/3})$. If $\lambda_i \in \tilde{V}_{s/3}(\lambda_{s/3})$ and the distance from λ_i to the boundary of $\tilde{V}_{s/3}(\lambda_{s/3})$ is not smaller than $3\bar{r}_{in}$, then encoder i determines that, for any other j, λ_j also belongs to $\tilde{V}_{s/3}(\lambda_{s/3})$. Therefore, we define $\mathcal{S}(\lambda_{s/3})$ as the set of points in $\tilde{V}_{s/3}(\lambda_{s/3})$ such that the distance to the boundary of $\tilde{V}_{s/3}(\lambda_{s/3})$ is smaller than $3\bar{r}_{in}$. Further, let $\mathcal{S} \triangleq \cup_{\lambda_{s/3}\in\Lambda_{s/3}}\mathcal{S}(\lambda_{s/3})$. Note that $\mathcal{S} \subseteq \mathcal{W}$. According to Lemma 1, if $\lambda_i \notin \mathcal{S}$, then for any $\lambda_j, j \in \{1,2,3\}\setminus\{i\}$, $Q_{s/3}(Q_f(\lambda_i)) = Q_{s/3}(Q_f(\lambda_j))$, when $x_i^n - x_j^n \in \mathcal{B}_{r_0}$. Next we describe in details how the encoder and decoder proceed. The encoder operation is illustrated in Figure 4.

Encoder. For $i = 1,2,3$, encoder i proceeds as follows. The source sequence x_i^n is first mapped to the nearest point in the central lattice, $\lambda_{c,i} \triangleq Q_c(x_i^n)$. Further, $\lambda_{c,i}$ is quantized to the nearest point in Λ_{in}, $\lambda_i \triangleq Q_{in}(\lambda_{c,i})$. Let $u_i \triangleq \lambda_{c,i} \bmod \Lambda_{in}$ and $\lambda_{s,i} \triangleq \beta_i(\lambda_i)$. Then the encoder outputs $\lambda_{s,i}$, u_i, a_i, where $a_i = 1$ if $\lambda_i \in \mathcal{W}$ and $a_i = 0$ otherwise. In addition, if $a_i = 1$, the encoder also outputs $\tilde{\lambda}_{f,i} \triangleq Q_f(\lambda_i) \bmod \Lambda_{s/3}$ and b_i, where $b_i = 1$ if $\lambda_i \in \mathcal{S}$ and $b_i = 0$ otherwise. Moreover, if $b_i = 1$, the encoder also transmits $\tau_i \triangleq Q_{s/3}(Q_f(\lambda_i)) \bmod \Lambda_s$. The first output, $\lambda_{s,i}$, will be utilized at the side decoder i. For this reason, it is compressed with an entropy encoder before being transmitted. Differently, u_1, u_2 and u_3 are employed at the central decoder only. Consequently, they can be compressed with a Slepian-Wolf encoder. Lastly, a_i, b_i, $\tilde{\lambda}_{f,i}$ and τ_i are needed only at the central decoder. Therefore, they also can be compressed with a Slepian-Wolf encoder. Nevertheless, we prefer to use entropy encoding for a_i, b_i and fixed length codes for τ_i and $\tilde{\lambda}_{f,i}$ to simplify the analysis, since, as we will see shortly, the rate overhead is negligible asymptotically.

Decoder. Side decoder i, for $i = 1,2,3$, outputs the reconstruction $\hat{x}_{s,i}^n \triangleq \lambda_{s,i}$. The central decoder restores all three values $\lambda_{s,1}$, $\lambda_{s,2}$ and $\lambda_{s,3}$, and additionally, $u_1, u_2, u_3, a_1, a_2, a_3$ and b_1, b_2, b_3, if applicable. The decoder first verifies whether the following inequality is satisfied

$$\|\lambda_{s,i} - \lambda_{s,j}\| \quad \leq \quad 2(5+2c_0)\bar{r}_s + 3\bar{r}_{in}, \tag{26}$$

for all $i,j \in \{1,2,3\}$. If condition (26) is violated for at least one pair (i,j) then the central decoder concludes that $x_j^n - x_i^n \notin \mathcal{B}_{r_0}$, and reconstructs source i using $\lambda_{s,i}$, i.e., $\hat{x}_{c,i}^n \triangleq \lambda_{s,i}$, for $i = 1,2,3$.

If inequality (26) holds for all pairs (i,j), then the central decoder assumes that $x_j^n - x_i^n \in \mathcal{B}_{r_0}$, for all pairs (i,j). For each $i = 1,2,3$, it computes an estimate of λ_i, denoted by $\hat{\lambda}_i$, and outputs the reconstruction $\hat{x}_{c,i}^n \triangleq \tilde{\lambda}_i + u_i$. For this the following are calculated first

$$\tilde{\lambda}_a \triangleq Q_{in}(u_1-u_2),\ \tilde{\lambda}_b \triangleq Q_{in}(u_1-u_3),\ \tilde{\lambda}_c \triangleq Q_{in}(u_2-u_3). \tag{27}$$

Next the decoder proceeds to compute $\hat{\lambda}_i$ based on the values of a_1, a_2 and a_3, and of $\tilde{\lambda}_{f,1}, \tilde{\lambda}_{f,2}, \tilde{\lambda}_{f,3}, b_1, b_2, b_3, \tau_1, \tau_2$ and τ_3 (where applicable), in accordance with the following cases.

This is the author's version of an article that has been published in this journal. Changes were made to this version by the publisher prior to publication.
The final version of record is available at http://dx.doi.org/10.1109/TCOMM.2020.2987565

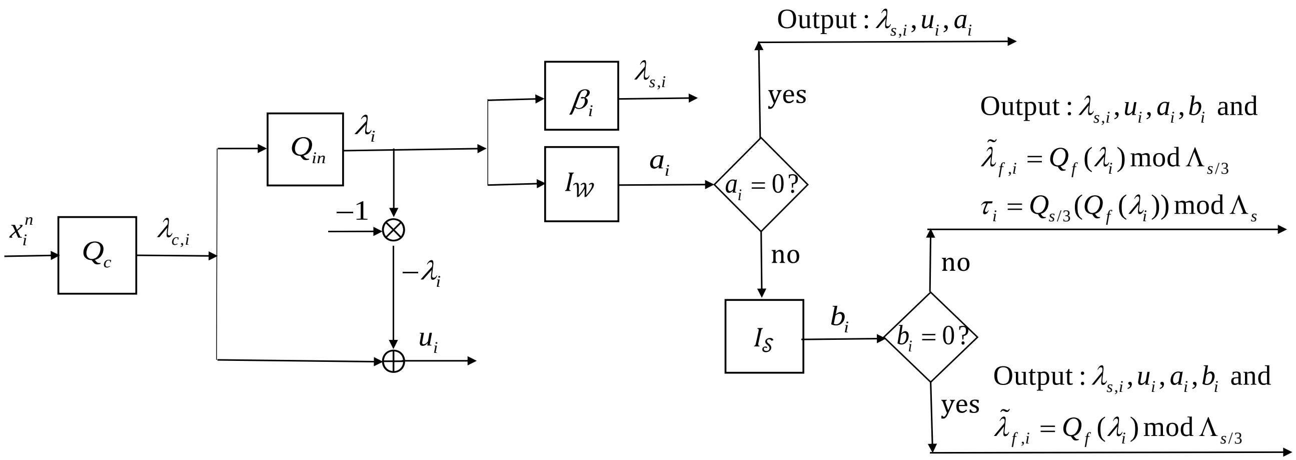

Fig. 4. Diagram illustrating the operation of encoder i, for $i = 1, 2, 3$. $I_{\mathcal{W}}$ and $I_{\mathcal{S}}$ denote the indicator functions of the sets $\mathcal{W}$ and $\mathcal{S}$, respectively.

1) If $a_1 = 0$ or $a_2 = 0$ or $a_3 = 0$ the decoder evaluates

$$\hat{\lambda}_{s/3} \triangleq \frac{1}{3}(\lambda_{s,1} + \lambda_{s,2} + \lambda_{s,3} + 3c_0^2\tilde{\lambda}_c), \tag{28}$$

$$\hat{\tau} \triangleq \hat{\lambda}_{s/3} \bmod \Lambda_s, \ \ \hat{\lambda}_s \triangleq Q_s(\hat{\lambda}_{s/3}), \tag{29}$$

$$\hat{\lambda}_f \triangleq \frac{1}{3c_0}(\lambda_{s,1} - \hat{\lambda}_s), \tag{30}$$

$$\hat{u}_{f,2} \triangleq \frac{1}{3c_0^2}(\lambda_{s,2} - \hat{\lambda}_s), \tag{31}$$

$$\hat{\lambda}_2 \triangleq \hat{\lambda}_s + \hat{\tau} + \hat{\lambda}_f + \hat{u}_{f,2}, \tag{32}$$

$$\hat{\lambda}_1 \triangleq \hat{\lambda}_2 - \tilde{\lambda}_a, \ \ \hat{\lambda}_3 \triangleq \hat{\lambda}_2 + \tilde{\lambda}_c. \tag{33}$$

2) If $a_1 = a_2 = a_3 = 1$ and $\tilde{\lambda}_{f,1} = \tilde{\lambda}_{f,2} = \tilde{\lambda}_{f,3}$ the decoder operates as in case 1.
3) If $a_1 = a_2 = a_3 = 1$, $\tilde{\lambda}_{f,1}, \tilde{\lambda}_{f,2}, \tilde{\lambda}_{f,3}$ are not all equal and $b_i = 0$ for at least one $i \in \{1, 2, 3\}$, then the decoder computes

$$\begin{aligned}\hat{\lambda}_{s/3} \triangleq \frac{1}{3}\Big(&\lambda_{s,1} + \lambda_{s,2} + \lambda_{s,3} + 3c_0(1-c_0)\tilde{\lambda}_{f,3} \\ &+ 3c_0^2(\tilde{\lambda}_{f,2} + \tilde{\lambda}_c) - 3c_0\tilde{\lambda}_{f,1}\Big),\end{aligned} \tag{34}$$

$$\hat{\lambda}_s \triangleq Q_s(\hat{\lambda}_{s/3}), \ \ \hat{\tau} \triangleq \hat{\lambda}_{s/3} \bmod \Lambda_s, \tag{35}$$

$$\hat{u}_{f,3} \triangleq \frac{1}{3c_0^2}(\hat{\lambda}_s + 3\hat{\tau} - 3c_0\tilde{\lambda}_{f,3} - \lambda_{s,3}), \tag{36}$$

$$\hat{\lambda}_3 \triangleq \hat{\lambda}_s + \hat{\tau} + \tilde{\lambda}_{f,i} + \hat{u}_{f,3}, \tag{37}$$

$$\hat{\lambda}_1 \triangleq \hat{\lambda}_3 - \tilde{\lambda}_b, \ \ \hat{\lambda}_2 \triangleq \hat{\lambda}_3 - \tilde{\lambda}_c. \tag{38}$$

4) If $a_1 = a_2 = a_2 = 1$ and $b_1 = b_2 = b_3 = 1$, then the decoder computes

$$\hat{\lambda}_{s_1} \triangleq \lambda_{s,1} - 3c_0\tilde{\lambda}_{f,1}, \ \ \hat{\lambda}_{s_2} \triangleq \hat{\lambda}_{s1} - Q_s(\tau_2 - \tau_1), \tag{39}$$

$$\hat{u}_{f,2} \triangleq \frac{1}{3c_0^2}(\lambda_{s,2} - \hat{\lambda}_{s_2}), \tag{40}$$

$$\hat{\lambda}_2 \triangleq \hat{\lambda}_{s_2} + \tau_2 + \tilde{\lambda}_{f,2} + \hat{u}_{f,2}, \tag{41}$$

$$\hat{\lambda}_1 \triangleq \hat{\lambda}_2 - \tilde{\lambda}_a, \ \ \hat{\lambda}_3 \triangleq \hat{\lambda}_2 + \tilde{\lambda}_c. \tag{42}$$

Remark 5. *It is worth pointing out that the proposed RDSC scheme has significant differences versus the scheme of [44]. The main difference stems from the use of the additional lattice Λ_f in the proposed design for three sources. As a consequence, more cases have to be considered at each encoder. More specifically, in [44] there are only two cases at each encoder (distinguished by one binary variable), while in the proposed work there are three cases at each encoder (distinguished by two binary variables). This also leads to the increase of the number of cases to be handled at the decoder from three in [44] to four in the proposed scheme.*

The following result essentially states that, if the three input sequences are at a distance of at most r_0 of one another, then the central decoder is able to refine the reconstructions to their most finely quantized representations, i.e., using the central lattice. The proof of the result can be found in Appendix A.

Proposition 1. *Let $x_i^n \in \mathbb{R}^n$, $\lambda_{c,i} \triangleq Q_c(x_i^n)$, $\lambda_i \triangleq Q_{in}(\lambda_{c,i})$, $u_i \triangleq \lambda_{c,i}$ mod Λ_{in}, $\lambda_{s,i} \triangleq \beta_i(\lambda_i)$, $\tilde{u}_{f,i} = \lambda_i$ mod Λ_f, $\tilde{\lambda}_{f,i} = Q_f(\lambda_i)$ mod $\Lambda_{s/3}$, $\tau_i \triangleq Q_{s/3}(Q_f(\lambda_i))$ mod Λ_s, and $\lambda_{s_i} \triangleq Q_s(Q_{s/3}(Q_f(\lambda_i))$ for $i = 1, 2, 3$. Then when $x_j^n - x_i^n \in B_{r_0}$, for $i, j \in \{1, 2, 3\}$, Slepian-Wolf decoding of u_1, u_2 and u_3 is successful, and c_0 is sufficiently large, we have $\hat{x}_{c,i}^n = \lambda_{c,i}$, for $i = 1, 2, 3$.*

VI. Conclusion

This work proposes a lattice-based coding scheme for robust distributed source coding for three correlated sources. We derive the expressions of the rates and distortions, for fixed lattice dimension, when the distortions at the individual decoders and the ratio between the distortions at the central and individual decoders approach 0. It is additionally shown that, when the sources are identical and Gaussian, the asymptotic performance of our scheme is very close to the theoretical bound of the quadratic symmetric Gaussian multiple description problem with central and individual decoders, with a gap of 0.069 bits in terms of rate per description. The proposed scheme can be extended in a straightforward manner to the case where the number of sources is greater than three.

Appendix A
Proof of Proposition 1

We first need the following lemma.

Lemma 2. *The following relation holds for $i = 1, 2, 3,$*

$$\bar{r}(\beta_i^{-1}(\mathbf{0})) \leq (5 + 2c_0)\bar{r}_s. \tag{43}$$

Proof: Notice that equation (22) implies that

$$\bar{r}(\beta_i^{-1}(\mathbf{0})) \leq \bar{r}(\mathcal{U}) + \bar{r}(\beta_i(\mathcal{U})). \tag{44}$$

From (19) one obtains that $\bar{r}(\mathcal{U}) \leq \bar{r}(\mathcal{T}) + \bar{r}(\mathcal{L}) + \bar{r}(\mathcal{F})$. Since $\mathcal{T} \subset V_s(\mathbf{0})$, $\mathcal{L} \subset V_{s/3}(\mathbf{0})$ and $\mathcal{F} \subset V_f(\mathbf{0})$, it further follows that $\bar{r}(\mathcal{U}) \leq \bar{r}_s + \bar{r}_{s/3} + \bar{r}_f \leq 2\bar{r}_s$. In addition, the definition of β_i implies that $\bar{r}(\beta_i(\mathcal{U})) \leq 3\bar{r}(\mathcal{T}) + 3c_0\bar{r}(\mathcal{L}) + 3c_0^2\bar{r}(\mathcal{F}) \leq 3\bar{r}_s + 3c_0\bar{r}_{s/3} + 3c_0^2\bar{r}_f$. Combining the above discussion with (44), $\bar{r}_{s/3} = \frac{1}{3}\bar{r}_s$, and $\bar{r}_f = \frac{1}{3c_0}\bar{r}_s$ leads to (43). ∎

Proof of Proposition 1: Let us assume that $x_j^n - x_i^n \in B_{r_0}$, for all $i, j \in \{1, 2, 3\}$. Let us also assume that the Slepian-Wolf decoder used at the central decoder recovers u_1, u_2 and u_3 correctly. We will first prove that condition (26) is fulfilled. Let us fix arbitrary $i \neq j, i, j \in \{1, 2, 3\}$. Notice that the shift invariant property (20) of β_k, combined with equality (22), implies that $\|\lambda - \beta_k(\lambda)\| \leq \bar{r}(\beta_k^{-1}(\mathbf{0}))$ for all $k \in \{1, 2, 3\}$ and $\lambda \in \Lambda_{in}$. This observation, together with the triangle inequality and Lemma 1, leads to $\|\lambda_{s,i} - \lambda_{s,j}\| \leq \|\lambda_{s,i} - \lambda_i\| + \|\lambda_i - \lambda_j\| + \|\lambda_j - \lambda_{s,j}\| \leq 2\bar{r}(\beta^{-1}(\mathbf{0})) + 3\bar{r}_{in}$, which together with (43) gives (26).

Using Lemma 1 and the fact that $\lambda_{c,k} = \lambda_k + u_k$, $k = 1, 2, 3$, we obtain that $r_{in} > \|\lambda_{c,i} - \lambda_{c,j}\| = \|u_i - u_j - (\lambda_j - \lambda_i)\|$, which, together with the fact that $\lambda_j - \lambda_i \in \Lambda_{in}$, implies that $u_i - u_j \in V_{in}(\lambda_j - \lambda_i)$, i.e., $\lambda_j - \lambda_i = Q_{in}(u_i - u_j)$. This further implies that $\tilde{\lambda}_a$, $\tilde{\lambda}_b$, $\tilde{\lambda}_c$ computed in (27) satisfy the equalities

$$\tilde{\lambda_a} = \lambda_2 - \lambda_1,\ \tilde{\lambda_b} = \lambda_3 - \lambda_1,\ \tilde{\lambda_c} = \lambda_3 - \lambda_2. \tag{45}$$

According to (18), we have

$$\lambda_i = \lambda_{s_i} + \tau_i + \tilde{\lambda}_{f,i} + \tilde{u}_{f,i},\ i = 1, 2, 3. \tag{46}$$

Moreover, since $\lambda_{s,i} = \beta_i(\lambda_i)$, for $i = 1, 2, 3$, one obtains that

$$\lambda_{s,1} = 3c_0\tilde{\lambda}_{f,1} + \lambda_{s_1}, \tag{47}$$
$$\lambda_{s,2} = 3c_0^2\tilde{u}_{f,2} + \lambda_{s_2}, \tag{48}$$
$$\lambda_{s,3} = 3\tau_3 - 3c_0\tilde{\lambda}_{f,3} - 3c_0^2\tilde{u}_{f,3} + \lambda_{s_3}. \tag{49}$$

Adding the three equations above, side by side, leads to

$$\begin{aligned}\lambda_{s,1} + \lambda_{s,2} + \lambda_{s,3} &= \lambda_{s_1} + \lambda_{s_2} + \lambda_{s_3} + 3\tau_3 \\ &+ 3c_0(\tilde{\lambda}_{f,1} - \tilde{\lambda}_{f,3}) + 3c_0^2(\tilde{u}_{f,2} - \tilde{u}_{f,3}).\end{aligned} \tag{50}$$

Recall that $\tilde{u}_{f,i} = \lambda_i - Q_f(\lambda_i)$, for all i, which together with (45) yields $\tilde{u}_{f,2} - \tilde{u}_{f,3} = -\tilde{\lambda}_c + Q_f(\lambda_3) - Q_f(\lambda_2)$. Suppose now that case 1 holds. Based on Lemma 1, it follows that $Q_f(\lambda_1) = Q_f(\lambda_2) = Q_f(\lambda_3)$. This further implies that $\tilde{u}_{f,2} - \tilde{u}_{f,3} = -\tilde{\lambda}_c$, $\tilde{\lambda}_{f,1} = \tilde{\lambda}_{f,2} = \tilde{\lambda}_{f,3}$, $\tau_1 = \tau_2 = \tau_3$ and $\lambda_{s_1} = \lambda_{s_2} = \lambda_{s_3}$. Then relation (50) leads to $\lambda_{s,1} + \lambda_{s,2} + \lambda_{s,3} = 3(\lambda_{s_1} + \tau_1) - 3c_0^2\tilde{\lambda}_c$. The above equality, together with (28), implies that $\hat{\lambda}_{s/3} = \lambda_{s_1} + \tau_1$. Combining this with (29) leads to $\hat{\tau} = \tau_1 = \tau_2 = \tau_3$ and $\hat{\lambda}_s = \lambda_{s_1} = \lambda_{s_2} = \lambda_{s_3}$. Now invoking (30), (31), (47) and (48), one further obtains $\hat{\lambda}_f = \tilde{\lambda}_{f,1} = \tilde{\lambda}_{f,2} = \tilde{\lambda}_{f,3}$ and $\hat{u}_{f,2} = \tilde{u}_{f,2}$. Employing further equations (32) and (46) leads to $\hat{\lambda}_2 = \lambda_2$, which together with (33) and (45) implies that $\hat{\lambda}_i = \lambda_i$, for $i = 1, 2, 3$.

Assume now that $a_1 = a_2 = a_3 = 1$. Consider arbitrary $i \neq j$, $i, j \in \{1, 2, 3\}$. Recall that, according to Lemma 1, $\|\lambda_i - \lambda_j\| < r_{in}$. Since $\Lambda_f = c_0\Lambda_{in}$, for c_0 sufficiently large, r_{in} is smaller than the smallest distance between non-adjacent Voronoi regions of Λ_f. This implies that λ_i and λ_j are either in the same or in adjacent Voronoi regions of Λ_f. Notice that $Q_f(\lambda_k) = \tilde{\lambda}_{f,k} + \tau_k + \lambda_{s_k}$, for any $k \in \{1, 2, 3\}$. Then, if $\tilde{\lambda}_{f,i} = \tilde{\lambda}_{f,j}$, it follows that $Q_f(\lambda_i) - Q_f(\lambda_j) = \tau_i + \lambda_{s_i} - \tau_j - \lambda_{s_j} \in \Lambda_{s/3} = c_0\Lambda_f$. This implies that $Q_f(\lambda_i)$ and $Q_f(\lambda_j)$ cannot be adjacent points of Λ_f. Therefore, it only remains the possibility that they are equal. This leads to $\tau_i + \lambda_{s_i} = \tau_j + \lambda_{s_j}$ and further to $\tau_i = \tau_j$ and $\lambda_{s_i} = \lambda_{s_j}$. Thus, the proof of case 2 carries on as in case 1.

Suppose now that case 3 holds. The fact that $b_i = 0$ and Lemma 1 imply that $Q_{s/3}(Q_f(\lambda_1)) = Q_{s/3}(Q_f(\lambda_2)) = Q_{s/3}(Q_f(\lambda_3))$, leading to $\lambda_{s_1} = \lambda_{s_2} = \lambda_{s_3}$ and $\tau_1 = \tau_2 = \tau_3$. Combining this with (46) and (45), one further obtains $\tilde{u}_{f,2} - \tilde{u}_{f,3} = -\tilde{\lambda}_c - \tilde{\lambda}_{f,2} + \tilde{\lambda}_{f,3}$. Plugging this in (50) yields $\lambda_{s,1} + \lambda_{s,2} + \lambda_{s,3} = 3(\lambda_{s_3} + \tau_3) + 3c_0(\tilde{\lambda}_{f,1} - \tilde{\lambda}_{f,3}) - 3c_0^2(\tilde{\lambda}_c + \tilde{\lambda}_{f,2} - \tilde{\lambda}_{f,3})$. The above equation, together with (34), leads to $\hat{\lambda}_{s/3} = \lambda_{s_3} + \tau_3$. Combining this with (35) gives that $\hat{\tau} = \tau_3$ and $\hat{\lambda}_s = \lambda_{s3}$. Equations (36) and (49) further lead to $\hat{u}_{f_3} = \tilde{u}_{f_3}$. This in conjunction with (37) and (46) implies $\hat{\lambda}_3 = \lambda_3$. Now one can readily invoke (45) to show that $\hat{\lambda}_i = \lambda_i$ for $i = 1, 2, 3$.

In order to address case 4, we need the following result.

Assertion 1: If $\lambda_{s/3} \in \Lambda_{s/3}$ and $V_{s/3}(\lambda_{s/3})$ is adjacent to $V_{s/3}(\mathbf{0})$, then $\lambda_{s/3} \in V_s(\mathbf{0})$.

Proof: Let $\lambda_{s/3} \in \Lambda_{s/3}$, then $3\lambda_{s/3} \in \Lambda_s$. Since $V_{s/3}(\lambda_{s/3})$ and $V_{s/3}(\mathbf{0})$ are adjacent, it follows that $V_s(3\lambda_{s/3})$ and $V_s(\mathbf{0})$ are adjacent. Then $\frac{3\lambda_{s/3}}{2}$ is on the boundary of $V_s(\mathbf{0})$. The point $\lambda_{s/3}$ is in the interior of the segment connecting $\mathbf{0}$ and $\frac{3\lambda_{s/3}}{2}$. Therefore, $\lambda_{s/3}$ is in the interior of $V_s(\mathbf{0})$. This concludes the proof of Assertion 1.

Now assume that case 4 holds. It can be easily verified that $Q_{s/3}(Q_f(\lambda_i)) = \tau_i + \lambda_{s_i}$, for any $i = 1, 2, 3$. Then, based on definition (25), it follows that $\lambda_i \in \tilde{V}_{s/3}(\tau_i + \lambda_{s_i})$, for $i = 1, 2, 3$. Since $\Lambda_{s/3} = c_0^2\Lambda_{in}$, for c_0 sufficiently large, r_{in} is smaller than the smallest distance between non-adjacent sets $\tilde{V}_{s/3}(\lambda_{s/3})$. According to Lemma 1, one has $\|\lambda_1 - \lambda_2\| < r_{in}$, therefore $\tilde{V}_{s/3}(\tau_1 + \lambda_{s_1})$ and $\tilde{V}_{s/3}(\tau_2 + \lambda_{s_2})$ are either identical or adjacent. This implies that $V_{s/3}(\lambda_{s_1} + \tau_1)$ and $V_{s/3}(\lambda_{s_2} + \tau_2)$ are either identical or adjacent, and further that $V_{s/3}(\lambda_{s_2} + \tau_2) - (\lambda_{s_1} + \tau_1))$ and $V_{s/3}(\mathbf{0})$ are either identical or adjacent. Using Assertion 1 one obtains that $\lambda_{s_2} + \tau_2 - (\lambda_{s_1} + \tau_1) \in V_s(\mathbf{0})$, leading to $\mathbf{0} = Q_s(\lambda_{s_2} - \lambda_{s_1} + \tau_2 - \tau_1) = \lambda_{s_2} - \lambda_{s_1} + Q_s(\tau_2 - \tau_1)$, i.e., $Q_s(\tau_2 - \tau_1) = \lambda_{s_1} - \lambda_{s_2}$. Combining the above with (39) and (47) implies that $\hat{\lambda}_{s_1} = \lambda_{s_1}$ and $\hat{\lambda}_{s_2} = \lambda_{s_2}$. Using further (40) and (48) leads to $\hat{u}_{f_2} = \tilde{u}_{f_2}$. Based on (41) and (46), the equality $\hat{\lambda}_2 = \lambda_2$ follows. By additionally exploiting (42) and (45), one can establish relations $\hat{\lambda}_i = \lambda_i$, for $i = 1, 2, 3$. With these observations, the proof is complete. ∎

APPENDIX B
PROOF OF THEOREM 1

The following lemma will be used extensively.

Lemma 3. *Let $\mathcal{S}_1$ and $\mathcal{S}_2$ be two finite subsets of $\mathbb{R}^n$. Then* $\sum_{\lambda_1\in\mathcal{S}_1}\sum_{\lambda_2\in\mathcal{S}_2}|\langle\lambda_1,\lambda_2\rangle|\le|\mathcal{S}_1||\mathcal{S}_2|\bar{r}(\mathcal{S}_1)\bar{r}(\mathcal{S}_2)$.

Proof: Based on the Cauchy-Schwarz inequality, one obtains

$$\begin{aligned}\sum_{\lambda_1\in\mathcal{S}_1}\sum_{\lambda_2\in\mathcal{S}_2}|\langle\lambda_1,\lambda_2\rangle| &\le \sum_{\lambda_1\in\mathcal{S}_1}\sum_{\lambda_2\in\mathcal{S}_2}\|\lambda_1\|\|\lambda_2\|\\ &\le \sum_{\lambda_1\in\mathcal{S}_1}\sum_{\lambda_2\in\mathcal{S}_2}\bar{r}(\mathcal{S}_1)\bar{r}(\mathcal{S}_2)\\ &= |\mathcal{S}_1||\mathcal{S}_2|\bar{r}(\mathcal{S}_1)\bar{r}(\mathcal{S}_2).\end{aligned}$$

■

A. Proof of Relation (7)

For each $\lambda_s\in\Lambda_s$ and $i=1,2,3$, let $\mathcal{A}_i(\lambda_s)\triangleq\{x_i^n|\hat{x}_{s,i}^n=\lambda_s\}$. Next, for every $\lambda\in\Lambda_{in}$, let $\mathcal{M}(\lambda)\triangleq\cup_{\lambda_c\in V_{in}(\lambda)\cap\Lambda_c}V_c(\lambda_c)$. Then $\mathcal{A}_i(\lambda_s)=\cup_{\lambda\in\beta_i^{-1}(\lambda_s)}\mathcal{M}(\lambda)$. It is obvious that $\mathcal{M}(\lambda)=\lambda+\mathcal{M}(\mathbf{0})$ for all $\lambda\in\Lambda$. Combining the above with equality (21) leads to

$$\mathcal{A}_i(\lambda_s)=\mathcal{A}_i(\mathbf{0})+\lambda_s,\quad\forall\lambda_s\in\Lambda_s. \tag{51}$$

Clearly, one has $d_{s,i}(\mathcal{L}^{(n,r_0)})=D(Q_{\mathcal{A}_i},X_i^n)$, where $Q_{\mathcal{A}_i}$ is the quantizer which mapping every source sequence $x_i^n\in\mathcal{A}_i(\lambda_s)$ to λ_s, for $\lambda_s\in\Lambda_s$. Now let us fix i. The rest of the proof will be divided in two parts. Part 1 shows that, assuming the existence of $\lim_{(6)}\frac{G(\mathcal{A}_i(\mathbf{0}))}{c_0^2}$, one has

$$\lim_{(6)}\frac{D(Q_{\mathcal{A}_i},X_i^n)}{c_0^2\nu_s^{\frac{2}{n}}}=\lim_{(6)}\frac{G(\mathcal{A}_i(\mathbf{0}))}{c_0^2}. \tag{52}$$

In Part 2 we evaluate $\lim_{(6)}\frac{G(\mathcal{A}_i(\mathbf{0}))}{c_0^2}$.

Part 1. This proof is similar to Part 1 of the proof of relation (23) in [44, Appendix C], which in turn employs ideas from the proof of [49, Lemma 1], but with some differences in the form of the expressions involved. Therefore, we will only mention the main steps, but provide the intermediate expressions in detail. The key idea of the proof is that, in the limit of (6), the pdf $f_{X_i^n}$ can be approximated by a density function which is uniform over every set $\mathcal{A}_i(\lambda_s)$. Specifically, let $\mathbf{c}\triangleq(\theta,c_0)$ and define the density function $f_{\mathbf{c}}:\mathbb{R}^n\to[0,\infty)$ as follows. For each $\lambda_s\in\Lambda_s$ and $x^n\in\mathcal{A}_i(\lambda_s)$, let

$$f_{\mathbf{c}}(x^n)=\frac{\mathbb{P}[X_i^n\in\mathcal{A}_i(\lambda_s)]}{\nu(\mathcal{A}_i(\lambda_s))}=\frac{1}{\nu(\mathcal{A}_i(\lambda_s))}\int_{\mathcal{A}_i(\lambda_s)}f_{X_i^n}(y^n)dy^n. \tag{53}$$

Let $X_{\mathbf{c}}^n$ denote the random variable with pdf $f_{\mathbf{c}}$. The following relation follows along the same lines as (72) in [44],

$$\begin{aligned}&\frac{1}{c_0^2\nu_s^{\frac{2}{n}}}|D(Q_{\mathcal{A}_i},X_{\mathbf{c}}^n)-D(Q_{\mathcal{A}_i},X_i^n)|\le\\ &\qquad\frac{\bar{r}(\mathcal{A}_i(\mathbf{0}))^2}{nc_0^2\nu_s^{\frac{2}{n}}}\int_{\mathbb{R}^n}|f_{\mathbf{c}}(x^n)-f_{X_i^n}(x^n)|dx^n.\end{aligned} \tag{54}$$

Further, since $\mathcal{A}_i(\mathbf{0})=\cup_{\lambda\in\beta_i(\mathbf{0})}(\lambda+\mathcal{M}(\mathbf{0}))$, we have $\bar{r}(\mathcal{A}_i(\mathbf{0}))\le\bar{r}(\beta_i^{-1}(\mathbf{0}))+\bar{r}(\mathcal{M}(\mathbf{0}))$, Combining this with (43), $\bar{r}_s=3c_0^2\theta\bar{r}_{in,0}$ and $\bar{r}(\mathcal{M}(\mathbf{0}))\le\bar{r}_{in}+\bar{r}_c\le2\bar{r}_{in}=2\theta\bar{r}_{in,0}$ gives $\bar{r}(\mathcal{A}_i(\mathbf{0}))\le9c_0^3\theta\bar{r}_{in,0}$, for c_0 large enough, which together with $\nu_s=(3c_0^2\theta)^n\nu_{in,0}$ implies that

$$\frac{\bar{r}(\mathcal{A}_i(\mathbf{0}))}{c_0\nu_s^{\frac{1}{n}}}\le\frac{9c_0^3\theta\bar{r}_{in,0}}{3c_o^3\theta\nu_{in,0}^{\frac{1}{n}}}\to\frac{3\bar{r}_{in,0}}{\nu_{in,0}^{\frac{1}{n}}} \tag{55}$$

as relations (6) hold. Further, relations (54) and (55) lead to $\lim_{(6)}\frac{1}{c_0^2\nu_s^{\frac{2}{n}}}|D(Q_{\mathcal{A}_i},X_{\mathbf{c}}^n)-D(Q_{\mathcal{A}_i},X_i^n)|=0$ as in [44, Proof of (77)]. Finally, the equality $D(Q_{\mathcal{A}_i},X_{\mathbf{c}}^n)=G(\mathcal{A}_i(\mathbf{0}))\nu_s^{\frac{2}{n}}$ follows as in [44, relations (78)]. The above two relations prove the claim.

Part 2. Recall that $\mathcal{A}_i(\mathbf{0})=\cup_{\lambda\in\beta_i^{-1}(\mathbf{0})}(\lambda+\mathcal{M}(\mathbf{0}))=\cup_{\lambda\in\mathcal{U}}(\lambda-\beta_i(\lambda)+\mathcal{M}(\mathbf{0}))$, where we have used relation (22). It can be readily verified that $\mathcal{M}(\mathbf{0})$ is a fundamental cell of Λ_{in}. Thus, one has $\nu(\mathcal{M}(\mathbf{0}))=\nu_{in}$. The next equality follows as in [44, Appendix C],

$$\begin{aligned}\int_{\mathcal{A}_i(\mathbf{0})}\|x^n\|^2dx^n=&\underbrace{|\mathcal{U}|\int_{\mathcal{M}(\mathbf{0})}\|x^n\|^2dx^n}_{T_1}\\ &+\underbrace{2\sum_{\lambda\in\mathcal{U}}\langle\int_{\mathcal{M}(\mathbf{0})}x^ndx^n,\lambda-\beta_i(\lambda)\rangle}_{T_{2,i}}\\ &+\underbrace{\nu_{in}\sum_{\lambda\in\mathcal{U}}\|\lambda-\beta_i(\lambda)\|^2}_{T_{3,i}}.\end{aligned}$$

Recall that $\nu(\mathcal{A}_i(\mathbf{0}))=\nu_s=M\nu_{in}$. Then

$$\begin{aligned}\frac{G(\mathcal{A}_i(\mathbf{0}))}{c_0^2}=&\frac{T_1}{nc_0^2(M\nu_{in})^{1+\frac{2}{n}}}+\frac{T_{2,i}}{nc_0^2(M\nu_{in})^{1+\frac{2}{n}}}\\ &+\frac{T_{3,i}}{nc_0^2(M\nu_{in})^{1+\frac{2}{n}}}.\end{aligned} \tag{56}$$

We first show that the first two terms in the right hand side of (56) go to 0 in the limit of (6). The proof is also similar to the counterpart in [44, Appendix C]. Let us start with the first term. Notice that $\int_{\mathcal{M}(\mathbf{0})}\|x^n\|^2dx^n\le(\bar{r}(\mathcal{M}(\mathbf{0})))^2\nu_{in}\le4\theta^2\bar{r}_{in,0}^2\nu_{in}$. Combining this with $|\mathcal{U}|=M$ and $\nu_{in}=\theta^n\nu_{in,0}$, we have

$$\begin{aligned}\frac{T_1}{nc_0^2(M\nu_{in})^{1+\frac{2}{n}}}&\le\frac{4M\theta^2\bar{r}_{in,0}^2\nu_{in}}{nc_0^2(M\nu_{in})^{1+\frac{2}{n}}}\\ &=\frac{4\bar{r}_{in,0}^2}{nc_0^2M^{\frac{2}{n}}\nu_{in,0}^{\frac{2}{n}}}\to0\text{ as (6) holds.}\end{aligned} \tag{57}$$

Further, it follows by the Cauchy-Schwarz inequality that

$$|T_{2,i}|\le2\int_{\mathcal{M}(\mathbf{0})}\|x^n\|dx^n\sum_{\lambda\in\mathcal{U}}\|\lambda-\beta_i(\lambda)\|.$$

Combining the above with $\int_{\mathcal{M}(\mathbf{0})}\|x^n\|dx^n\le\bar{r}(\mathcal{M}(\mathbf{0}))\nu_{in}\le\theta\bar{r}_{in,0}\nu_{in}$, $\sum_{\lambda\in\mathcal{U}}\|\lambda-\beta_i(\lambda)\|\le M\bar{r}(\beta_i^{-1}(\mathbf{0}))$, relation (43) and $\bar{r}_s=3c_0^2\theta\bar{r}_{in,0}$, one can readily show that, for sufficiently large c_0, $|T_{2,i}| \leq 36c_0^3\theta^2\nu_{in}M\bar{r}_{in,0}^2$. The above relation, together with $M = (3c_0^2)^n$, implies

$$\frac{|T_{2,i}|}{nc_0^2(M\nu_{in})^{1+\frac{2}{n}}} \leq \frac{36c_0^3\theta^2\nu_{in}M\bar{r}_{in,0}^2}{nc_0^2M^{1+\frac{2}{n}}\nu_{in}\theta^2\nu_{in,0}^{\frac{2}{n}}} = \frac{4\bar{r}_{in,0}^2}{nc_0^3\nu_{in,0}^{\frac{2}{n}}} \to 0 \text{ as (6) holds.} \tag{58}$$

Let us evaluate now $\frac{T_{3,i}}{\nu_{in}}$. From now on the similarity with the proof in [44] breaks down due to the more complex definition of the mappings β_i in the current work. We will discuss separately the cases $i = 1$, $i = 2$ and $i = 3$. Recall that $\mathcal{U} \triangleq \{\tau + \tilde{\lambda}_f + \tilde{u}_f | \tau \in \mathcal{T}, \tilde{u}_f \in \mathcal{F}, \tilde{\lambda}_f \in \mathcal{L}\}$. Notice that, if $\lambda \in \mathcal{U}$, then $Q_s(Q_{s/3}(Q_f(\lambda))) = \mathbf{0}$. Then $\lambda_s = \mathbf{0}$ in (17). Using now (17) and (18), one obtains that

$$\begin{aligned}\frac{T_{3,1}}{\nu_{in}} &= \sum_{\lambda\in\mathcal{U}} \|\lambda - 3c_0\tilde{\lambda}_f\|^2 \\ &= \sum_{\lambda\in\mathcal{U}} \left(\|(1-3c_0)(\tilde{\lambda_f})\|^2 + \|\tilde{u}_f\|^2 + \|\tau\|^2\right) \\ &\quad + \sum_{\lambda\in\mathcal{U}} \left(2(1-3c_0)\langle\tilde{\lambda}_f,\tau\rangle + 2(1-3c_0)\langle\tilde{\lambda}_f,\tilde{u}_f\rangle + 2\langle\tau,\tilde{u}_f\rangle\right) \\ &= \sum_{\tau\in\mathcal{T}}\sum_{\tilde{\lambda}_f\in\mathcal{L}}\sum_{\tilde{u}_f\in\mathcal{F}} (1-3c_0)^2\|\tilde{\lambda}_f\|^2 + \sum_{\tau\in\mathcal{T}}\sum_{\tilde{\lambda}_f\in\mathcal{L}}\sum_{\tilde{u}_f\in\mathcal{F}} \|\tilde{u}_f\|^2 \\ &\quad + \sum_{\tau\in\mathcal{T}}\sum_{\tilde{\lambda}_f\in\mathcal{L}}\sum_{\tilde{u}_f\in\mathcal{F}} \|\tau\|^2 \\ &\quad + 2(1-3c_0)\sum_{\tau\in\mathcal{T}}\sum_{\tilde{\lambda}_f\in\mathcal{L}}\sum_{\tilde{u}_f\in\mathcal{F}} \langle\tilde{u}_f,\tilde{\lambda}_f\rangle \\ &\quad + 2(1-3c_0)\sum_{\tau\in\mathcal{T}}\sum_{\tilde{\lambda}_f\in\mathcal{L}}\sum_{\tilde{u}_f\in\mathcal{F}} \langle\tilde{\lambda}_f,\tau\rangle \\ &\quad + 2\sum_{\tau\in\mathcal{T}}\sum_{\tilde{\lambda}_f\in\mathcal{L}}\sum_{\tilde{u}_f\in\mathcal{F}} \langle\tilde{u}_f,\tau\rangle.\end{aligned} \tag{59}$$

Consider the following quantities:

$$T_2 \triangleq \frac{\sum_{\tau\in\mathcal{T}}\sum_{\tilde{\lambda}_f\in\mathcal{L}}\sum_{\tilde{u}_f\in\mathcal{F}}\|\tilde{\lambda}_f\|^2}{nc_0^2M^{1+\frac{2}{n}}\nu_{in}^{\frac{2}{n}}},\ T_3 \triangleq \frac{\sum_{\tau\in\mathcal{T}}\sum_{\tilde{\lambda}_f\in\mathcal{L}}\sum_{\tilde{u}_f\in\mathcal{F}}\|\tilde{u}_f\|^2}{nc_0^2M^{1+\frac{2}{n}}\nu_{in}^{\frac{2}{n}}}, \tag{60}$$

$$T_4 \triangleq \frac{\sum_{\tau\in\mathcal{T}}\sum_{\tilde{\lambda}_f\in\mathcal{L}}\sum_{\tilde{u}_f\in\mathcal{F}}\|\tau\|^2}{nc_0^2M^{1+\frac{2}{n}}\nu_{in}^{\frac{2}{n}}},\ T_5 \triangleq \frac{\sum_{\tau\in\mathcal{T}}\sum_{\tilde{\lambda}_f\in\mathcal{L}}\sum_{\tilde{u}_f\in\mathcal{F}}\langle\tilde{u}_f,\tilde{\lambda}_f\rangle}{nc_0^2M^{1+\frac{2}{n}}\nu_{in}^{\frac{2}{n}}}, \tag{61}$$

$$T_6 \triangleq \frac{\sum_{\tau\in\mathcal{T}}\sum_{\tilde{\lambda}_f\in\mathcal{L}}\sum_{\tilde{u}_f\in\mathcal{F}}\langle\tilde{\lambda}_f,\tau\rangle}{nc_0^2M^{1+\frac{2}{n}}\nu_{in}^{\frac{2}{n}}},\ T_7 \triangleq \frac{\sum_{\tau\in\mathcal{T}}\sum_{\tilde{\lambda}_f\in\mathcal{L}}\sum_{\tilde{u}_f\in\mathcal{F}}\langle\tilde{u}_f,\tau\rangle}{nc_0^2M^{1+\frac{2}{n}}\nu_{in}^{\frac{2}{n}}}. \tag{62}$$

Relation (59) leads to

$$\frac{T_{3,1}}{nc_0^2(M\nu_{in})^{1+\frac{2}{n}}} = (1-3c_0)^2T_2 + T_3 + T_4 + 2(1-3c_0)T_5 + 2(1-3c_0)T_6 + 2T_7. \tag{63}$$

The following relations will be used extensively $M = 3^nc_0^{2n}$, $\nu_f = c_0^n\nu_{in}$, $\nu_{s/3} = c_0^{2n}\nu_{in}$, $\nu_s = 3^nc_0^{2n}\nu_{in}$, $|\mathcal{T}| = 3^n$, $|\mathcal{L}| = c_0^n$, $|\mathcal{F}| = c_0^n$, $\bar{r}_f = c_0\theta\bar{r}_{in,0}$ and $\bar{r}_{s/3} = c_0^2\theta\bar{r}_{in,0}$, $\bar{r}_s = 3c_0^2\theta\bar{r}_{in,0}$, $\nu_{in} = \theta^n\nu_{in,0}$. Based on Lemma 7 in [44], one obtains

$$\begin{aligned}T_2 &= \frac{nM}{9nMc_0^6\nu_{in}^{\frac{2}{n}}}\left(G(\mathcal{C}_{\Lambda_{s/3}:\Lambda_f})c_0^4\nu_{in}^{\frac{2}{n}} - G_fc_0^2\nu_{in}^{\frac{2}{n}}\right) \\ &= \frac{1}{9c_0^2}\left(G(\mathcal{C}_{\Lambda_{s/3}:\Lambda_f}) - \frac{1}{c_0^2}G_f\right),\end{aligned} \tag{64}$$

$$\begin{aligned}T_3 &= \frac{nM}{9nMc_0^6\nu_{in}^{\frac{2}{n}}}\left(G(\mathcal{C}_{\Lambda_f:\Lambda_{in}})c_0^2\nu_{in}^{\frac{2}{n}} - G_{in}\nu_{in}^{\frac{2}{n}}\right) \\ &= \frac{1}{9c_0^4}\left(G(\mathcal{C}_{\Lambda_f:\Lambda_{in}}) - \frac{1}{c_0^2}G_{in}\right),\end{aligned} \tag{65}$$

$$\begin{aligned}T_4 &= \frac{nM}{9nMc_0^6\nu_{in}^{\frac{2}{n}}}\left(9G(\mathcal{C}_{\Lambda_s:\Lambda_{s/3}})c_0^4\nu_{in}^{\frac{2}{n}} - G_{s/3}c_0^4\nu_{in}^{\frac{2}{n}}\right) \\ &= \frac{1}{c_0^2}\left(G(\mathcal{C}_{\Lambda_s:\Lambda_{s/3}}) - \frac{1}{9}G_{s/3}\right).\end{aligned} \tag{66}$$

Note that scaling preserves the normalized second moment. Therefore, one has $G_s = G_{s/3} = G_f$. This result, in conjunction with Lemma 8 in [44], implies that

$$\lim_{(6)} G(\mathcal{C}_{\Lambda_{s/3}:\Lambda_f}) = \lim_{(6)} G(\mathcal{C}_{\Lambda_f:\Lambda_{in}}) = \lim_{(6)} G(\mathcal{C}_{\Lambda_s:\Lambda_{s/3}}) = G_s. \tag{67}$$

Further, Lemma 3, together with $\bar{r}(\mathcal{F}) \leq \bar{r}_f$, $\bar{r}(\mathcal{L}) \leq \bar{r}_{s/3}$ and $\bar{r}(\mathcal{T}) \leq \bar{r}_s$, leads to

$$|T_5| \leq \frac{\sum_{\tau\in\mathcal{T}}\sum_{\tilde{\lambda}_f\in\mathcal{L}}\sum_{\tilde{u}_f\in\mathcal{F}}|\langle\tilde{u}_f,\tilde{\lambda}_f\rangle|}{nc_0^2M^{1+\frac{2}{n}}\nu_{in}^{\frac{2}{n}}} \leq \frac{M\bar{r}_f\bar{r}_{s/3}}{nc_0^2M^{1+\frac{2}{n}}\nu_{in}^{\frac{2}{n}}} = \frac{\bar{r}_{in,0}^2}{9nc_0^3\nu_{in,0}^{\frac{2}{n}}}, \tag{68}$$

$$|T_6| \leq \frac{\sum_{\tau\in\mathcal{T}}\sum_{\tilde{\lambda}_f\in\mathcal{L}}\sum_{\tilde{u}_f\in\mathcal{F}}|\langle\tilde{\lambda}_f,\tau\rangle|}{nc_0^2M^{1+\frac{2}{n}}\nu_{in}^{\frac{2}{n}}} \leq \frac{M\bar{r}_{s/3}\bar{r}_s}{nc_0^2M^{1+\frac{2}{n}}\nu_{in}^{\frac{2}{n}}} = \frac{\bar{r}_{in,o}^2}{3nc_0^2\nu_{in,0}^{\frac{2}{n}}}, \tag{69}$$

$$|T_7| \leq \frac{\sum_{\tau\in\mathcal{T}}\sum_{\tilde{\lambda}_f\in\mathcal{L}}\sum_{\tilde{u}_f\in\mathcal{F}}|\langle\tilde{u}_f,\tau\rangle|}{nc_0^2M^{1+\frac{2}{n}}\nu_{in}^{\frac{2}{n}}} \leq \frac{M\bar{r}_f\bar{r}_s}{nc_0^2M^{1+\frac{2}{n}}\nu_{in}^{\frac{2}{n}}} = \frac{\bar{r}_{in,o}^2}{3nc_0^3\nu_{in,0}^{\frac{2}{n}}}. \tag{70}$$

Based on relations (65)-(70), one obtains that

$$\begin{aligned}\lim_{(6)} T_3 &= \lim_{(6)} T_4 = \lim_{(6)} 2(1-3c_0)T_5 \\ &= \lim_{(6)} 2(1-3c_0)T_6 = \lim_{(6)} 2T_7 = 0.\end{aligned} \tag{71}$$

Further, relation (64) implies that $\lim_{(6)}(1-3c_0)^2T_2 = G_s$. Combining the above relation with (63) and (71) gives

$$\lim_{(6)} \frac{T_{3,1}}{nc_o^2M^{1+\frac{2}{n}}\nu_{in}^{\frac{2}{n}+1}} = G_s. \tag{72}$$

This is the author's version of an article that has been published in this journal. Changes were made to this version by the publisher prior to publication.
The final version of record is available at http://dx.doi.org/10.1109/TCOMM.2020.2987565

Let us evaluate now $\frac{T_{3,2}}{\nu_{in}}$.

$$\begin{aligned}\frac{T_{3,2}}{\nu_{in}} &= \sum_{\lambda\in\mathcal{U}} \|\lambda - 3c_0^2\tilde{u}_f\|^2 \\ &= \sum_{\lambda\in\mathcal{U}} \Big(\|(1-3c_0^2)\tilde{u}_f\|^2 + \|\tilde{\lambda}_f\|^2 + \|\tau\|^2\Big) \\ &\quad + \sum_{\lambda\in\mathcal{U}} \Big(2\langle\tilde{\lambda}_f,\tau\rangle + 2(1-3c_0^2)\langle\tilde{u}_f,\tilde{\lambda}_f\rangle \\ &\quad + (1-3c_0^2)\langle\tilde{u}_f,\tau\rangle\Big).\end{aligned}$$

The above equality, together with (60)-(62), leads to

$$\begin{aligned}\frac{T_{3,2}}{nc_o^2(M\nu_{in})^{1+\frac{2}{n}}} &= T_2 + (1-3c_0^2)^2T_3 + T_4 + 2(1-3c_0^2)T_5 \\ &\quad + 2T_6 + 2(1-3c_0^2)T_7. \end{aligned} \tag{73}$$

Using (65) and (67), one obtains

$$\lim_{(6)}(1-3c_0^2)^2T_3 = G_s. \tag{74}$$

From (64) and (66)-(70) it follows that

$$\begin{aligned}\lim_{(6)} T_2 &= \lim_{(6)} T_4 = \lim_{(6)} 2(1-3c_0^2)T_5 \\ &= \lim_{(6)} T_6 = \lim_{(6)} 2(1-3c_0^2)T_7 = 0. \end{aligned} \tag{75}$$

Relations (73)-(75) imply that

$$\lim_{(6)} \frac{T_{3,2}}{nc_0^2M^{1+\frac{2}{n}}\nu_{in}^{\frac{2}{n}+1}} = G_s. \tag{76}$$

Let us evaluate now $\frac{T_{3,3}}{\nu_{in}}$.

$$\begin{aligned}\frac{T_{3,3}}{\nu_{in}} &= \sum_{\lambda\in\mathcal{U}} \|\lambda - 3\tau + 3c_0\tilde{\lambda}_f + 3c_0^2\tilde{u}_f\|^2 \\ &= \sum_{\lambda\in\mathcal{U}} \Big(\|(1+3c_0)(\tilde{\lambda_f})\|^2 + \|(1+3c_0^2)\tilde{u}_f\|^2 + \|2\tau\|^2\Big) \\ &\quad + \sum_{\lambda\in\mathcal{U}} \Big(-4(1+3c_0)\langle\tilde{\lambda}_f,\tau)\rangle \\ &\qquad + 2(1+3c_0)(1+3c_0^2)\langle\tilde{u}_f,\tilde{\lambda}_f)\rangle \\ &\qquad - 4(1+3c_0^2)\langle\tilde{u}_f,\tau)\rangle\Big).\end{aligned}$$

Invoking (60)-(62) yields

$$\begin{aligned}\frac{T_{3,3}}{nc_0^2(M\nu_{in})^{1+\frac{2}{n}}} &= (1+3c_0)^2T_2 + (1+3c_0^2)^2T_3 \\ &\quad + 4T_4 + 2(1+3c_0)(1+3c_0^2)T_5 \\ &\quad - 4(1+3c_0)T_6 - 4(1+3c_0^2)T_7. \end{aligned} \tag{77}$$

It follows by (64), (65) and (67) that

$$\lim_{(6)}(1+3c_0)^2T_2 = \lim_{(6)}(1+3c_0^2)^2T_3 = G_s. \tag{78}$$

Further, according to (66), (69) and (70) one has

$$\lim_{(6)} T_4 = \lim_{(6)}(1+3c_0)T_6 = \lim_{(6)}(1+3c_0^2)T_7 = 0. \tag{79}$$

Next we prove that

$$\lim_{(6)}(1+3c_0)(1+3c_0^2)T_5 = 0. \tag{80}$$

For this, we need first to introduce more notation. Let $\mathcal{F}_b$ denote the set of points which are in $\mathcal{F}$ and on the boundary of $V_f(\mathbf{0})$ and let $\mathcal{L}_b$ denote the set of points which are in $\mathcal{L}$ and on the boundary of $V_{s/3}(\mathbf{0})$. Moreover, let $M_b = |\mathcal{F}_b|$ and $N_b = |\mathcal{L}_b|$. Note that $\mathcal{F}\setminus\mathcal{F}_b$ is symmetric about the origin. Thus, $\sum_{\tilde{u}_f\in\mathcal{F}\setminus\mathcal{F}_b}\tilde{u}_f = \mathbf{0}$. Likewise, $\sum_{\tilde{\lambda}_f\in\mathcal{L}\setminus\mathcal{L}_b}\tilde{\lambda}_f = \mathbf{0}$. Then based on the linearity of the scalar product, it follows that

$$\sum_{\tau\in\mathcal{T}}\sum_{\tilde{\lambda}_f\in\mathcal{L}}\sum_{\tilde{u}_f\in\mathcal{F}}\langle\tilde{u}_f,\tilde{\lambda}_f\rangle = \sum_{\tau\in\mathcal{T}}\sum_{\tilde{\lambda}_f\in\mathcal{L}_b}\sum_{\tilde{u}_f\in\mathcal{F}_b}\langle\tilde{u}_f,\tilde{\lambda}_f\rangle.$$

Thus, one obtains

$$\begin{aligned}\left|\sum_{\tau\in\mathcal{T}}\sum_{\tilde{\lambda}_f\in\mathcal{L}}\sum_{\tilde{u}_f\in\mathcal{F}}\langle\tilde{u}_f,\tilde{\lambda}_f\rangle\right| &= \left|\sum_{\tau\in\mathcal{T}}\sum_{\tilde{\lambda}_f\in\mathcal{L}_b}\sum_{\tilde{u}_f\in\mathcal{F}_b}\langle\tilde{u}_f,\tilde{\lambda}_f\rangle\right| \\ &\le \sum_{\tau\in\mathcal{T}}\sum_{\tilde{\lambda}_f\in\mathcal{L}_b}\sum_{\tilde{u}_f\in\mathcal{F}_b}|\langle\tilde{u}_f,\tilde{\lambda}_f\rangle| \\ &\le 3^nN_bM_b\bar{r}_f\bar{r}_{s/3},\end{aligned}$$

where the last inequality follows according to Lemma 3. Using further $\bar{r}_f = c_0\theta\bar{r}_{in,0}$ and $\bar{r}_{s/3} = c_0^2\theta\bar{r}_{in,0}$ leads to

$$|(1+3c_0)(1+3c_0^2)T_5| \le \frac{(1+3c_0)(1+3c_0^2)\bar{r}_{in,0}^2}{9nc_0^3\nu_{in,0}^{\frac{2}{n}}}\frac{3^nN_b}{3^nc_0^n}\frac{M_b}{c_0^n}. \tag{81}$$

Clearly, the first factor on the right hand side of the above relation is bounded. Next we will show that $\frac{N_b}{c_0^n} \to 0$ and $\frac{M_b}{c_0^n} \to 0$ as (6) holds, which, together with (81), implies (80).

For this, note first that $\frac{N_b}{c_0^n} = \frac{N_b\nu_f}{\nu_{s/3}}$. Now denote $\mathcal{N} \triangleq \cup_{\tilde{\lambda}_f\in\mathcal{L}_b}V_f(\tilde{\lambda}_f)$. It can be easily verified that

$$\mathcal{N} \subseteq \phi_1V_{s/3}(\mathbf{0}) \setminus \phi_2V_{s/3}(\mathbf{0}),$$

where $\phi_1 = 1 + \frac{\bar{r}_f}{\bar{r}_{s/3}}$ and $\phi_2 = 1 - \frac{\bar{r}_f}{\bar{r}_{s/3}}$. This implies that $N_b\nu_f = \nu(\mathcal{N}) \le (\phi_1^n - \phi_2^n)\nu_{s/3}$. Now let us show that $\lim_{(6)}(\phi_1^n - \phi_2^n) = 0$. Note that

$$\begin{aligned}(\phi_1^n - \phi_2^n) &= (\phi_1-\phi_2)(\phi_1^{n-1} + \phi_1^{n-2}\phi_2 + \cdots + \phi_2^{n-1}) \\ &\le (\phi_1-\phi_2)n\phi_1^{n-1}.\end{aligned}$$

Since $\phi_1^{n-1} \to 1$ as (6) holds, it is sufficient to show that $(\phi_1 - \phi_2) \to 0$ as (6) holds. We have

$$\phi_1 - \phi_2 = 1 + \frac{\bar{r}_f}{\bar{r}_{s/3}} - 1 + \frac{\bar{r}_f}{\bar{r}_{s/3}} = \frac{2\theta c_0\bar{r}_{in,0}}{c_0^2\theta\bar{r}_{in,0}} = \frac{2}{c_0} \to 0 \tag{82}$$

as (6) holds. We conclude that $\lim_{(6)}\frac{N_b}{c_0^n} = 0$. Similarly, it can be shown that $\lim_{(6)}\frac{M_b}{c_0^n} = \lim_{(6)}\frac{M_b\nu_{in}}{\nu_f} = 0$. Consequently, relation (80) is valid. Relations (77)-(80) imply that

$$\lim_{(6)}\frac{T_{3,3}}{nc_0^2M^{1+\frac{2}{n}}\nu_{in}^{\frac{2}{n}+1}} = 2G_s. \tag{83}$$

Finally, relations (56)-(58), (72), (76) and (83) lead to $\lim_{(6)}\frac{G(\mathcal{A}_1(\mathbf{0}))}{c_0^2} = \lim_{(6)}\frac{G(\mathcal{A}_2(\mathbf{0}))}{c_0^2} = G_s$ and $\lim_{(6)}\frac{G(\mathcal{A}_3(\mathbf{0}))}{c_0^2} = 2G_s$, which concludes Part 2. Combining Part 1 and Part 2 leads to (7).

B. Proof of Relations (8)

Denote $\Delta_{i,sup} \triangleq \sup_{x_i^n \in \mathbb{R}^n} \|x_i^n - \hat{x}_{c,i}^n\|$, for $i = 1, 2, 3$. The following result will be needed.

Lemma 4. *There is some constant κ_1 such that for c_0 sufficiently large, one has*

$$\Delta_{i,sup} \leq \kappa_1 c_0 \nu_s^{\frac{1}{n}}, \ i = 1, 2, 3.$$

Proof: Assume that $c_0 \geq 5$. According to equation (43), for $i = 1, 2, 3$, one has

$$\bar{r}(\beta_i^{-1}(\mathbf{0})) \leq 3c_o \bar{r}_s. \tag{84}$$

Let $x_i^n \in \mathbb{R}^n$ and consider the notation in Proposition 1. Using the fact that $\lambda_{c,i} = \lambda_i + u_i$ and the triangle inequality, one obtains

$$\begin{aligned}\|x_i^n - \hat{x}_{c,i}^n\| &= \|x_i^n - \lambda_{c,i} + u_i + \lambda_i - \hat{x}_{c,i}^n\| \\ &\leq \|x_{c,i}^n - \lambda_{c,i}\| + \|u_i\| + \|\lambda_i - \hat{x}_{c,i}^n\| \\ &\leq \bar{r}_c + \bar{r}_{in} + \|\lambda_i - \hat{x}_{c,i}^n\| \\ &\leq \bar{r}_s + \|\lambda_i - \hat{x}_{c,i}^n\|. \end{aligned} \tag{85}$$

If condition (26) is violated, then $\hat{x}_{c,i}^n = \lambda_{s,i}$, leading to $\|\lambda_i - \hat{x}_{c,i}^n\| = \|\lambda_i - \lambda_{s,i}\| \leq \bar{r}(\beta_i^{-1}(\mathbf{0})) \leq 3c_0\bar{r}_s$. By combining this with (85), one further obtains that $\|x_i^n - \hat{x}_{c,i}^n\| \leq (3c_0+1)\bar{r}_s \leq 4c_0\bar{r}_s$.

Consider now the situation when condition (26) is obeyed and case 1 is in effect, i.e., $a_1 = 0$ or $a_2 = 0$ or $a_3 = 0$. Recall that $\hat{x}_{c,i}^n = \tilde{\lambda}_i + u_i$, where $\tilde{\lambda}_i$ is evaluated by the decoder. Then

$$\|\lambda_i - \hat{x}_{c,i}^n\| \leq \|\lambda_i - \tilde{\lambda}_i\| + \|u_i\| \leq \|\lambda_i - \tilde{\lambda}_i\| + \bar{r}_{in}. \tag{86}$$

Let us consider $i = 2$. Using (32) and the triangle inequality then invoking (30) and (31), one obtains

$$\begin{aligned}\|\lambda_2 - \tilde{\lambda}_2\| &\leq \|\lambda_2 - \tilde{\lambda}_s\| + \|\tilde{\tau}\| + \|\bar{\tilde{\lambda}}_f\| + \|\bar{\tilde{u}}_{f,2}\| \\ &\leq \|\lambda_2 - \lambda_{s,2}\| + \|\lambda_{s,2} - \tilde{\lambda}_s\| + \|\tilde{\tau}\| \\ &\quad + \frac{1}{3c_0}\|\lambda_{s,1} - \tilde{\lambda}_s\| + \frac{1}{3c_0^2}\|\lambda_{s,2} - \tilde{\lambda}_s\|.\end{aligned}$$

Applying further $\|\lambda_2 - \lambda_{s,2}\| \leq \bar{r}(\beta_i^{-1}(\mathbf{0})) \leq 3c_0\bar{r}_s$, $\|\tilde{\tau}\| \leq \bar{r}_s$, $\frac{1}{3c_0} \leq 1$ and $\frac{1}{3c_0^2} \leq 1$ leads to

$$\|\lambda_2 - \tilde{\lambda}_2\| \leq 3c_0\bar{r}_s + \|\lambda_{s,1} - \tilde{\lambda}_s\| + 2\|\lambda_{s,2} - \tilde{\lambda}_s\|. \tag{87}$$

The relation $\tilde{\lambda}_s = \tilde{\lambda}_{s/3} - \tilde{\tau}$ (from (29)), together with the triangle inequality, implies

$$\|\lambda_{s,j} - \tilde{\lambda}_s\| \leq \|\lambda_{s,j} - \tilde{\lambda}_{s/3}\| + \|\tilde{\tau}\| \leq \|\lambda_{s,j} - \tilde{\lambda}_{s/3}\| + \bar{r}_s, \tag{88}$$

for $j = 1, 2, 3$. Combining (28) with the triangle inequality yields

$$\|\lambda_{s,1} - \tilde{\lambda}_{s/3}\| \leq \frac{1}{3}\|\lambda_{s,1} - \lambda_{s,2}\| + \frac{1}{3}\|\lambda_{s,1} - \lambda_{s,3}\| + c_0^2\|\tilde{\lambda}_c\|. \tag{89}$$

According to (26), one has $\|\lambda_{s,1} - \lambda_{s,j}\| \leq 6c_0\bar{r}_s + 3\bar{r}_{in}$. Plugging this in (89) leads to

$$\|\lambda_{s,1} - \tilde{\lambda}_{s/3}\| \leq 4c_0\bar{r}_s + 2\bar{r}_{in} + c_0^2\|\tilde{\lambda}_c\|. \tag{90}$$

Now we will derive an upper bound for $\|\tilde{\lambda}_c\|$. Note that

$$\tilde{\lambda}_c = Q_{in}(u_2 - u_3) = (u_2 - u_3) - (u_2 - u_3) \bmod Q_{in}.$$

Then

$$\|\tilde{\lambda}_c\| \leq \|u_2\| + \|u_3\| + \|(u_2 - u_3) \bmod Q_{in}(u_1 - u_2)\| \leq 3\bar{r}_{in}. \tag{91}$$

Plugging (91) in (90), then (90) in (88) and using the fact that $\bar{r}_s = 3c_0^2\bar{r}_{in}$ gives

$$\|\lambda_{s,1} - \tilde{\lambda}_s\| \leq 4c_0\bar{r}_s + 2\bar{r}_{in} + 2\bar{r}_s \leq 5c_0\bar{r}_s. \tag{92}$$

Similarly, one obtains $\|\lambda_{s,2} - \tilde{\lambda}_s\| \leq 5c_0\bar{r}_s$. Plugging the previous inequality and (92) in (87) yields $\|\lambda_2 - \tilde{\lambda}_2\| \leq 18c_0\bar{r}_s$. By combining the above inequality with (85) and (86), we have

$$\|x_1^n - \hat{x}_{c,1}^n\| \leq \bar{r}_s + 18c_0\bar{r}_s + \bar{r}_{in} \leq 19c_0\bar{r}_s,$$

for c_0 sufficiently large. The proof for the rest of the cases proceeds similarly. ∎

Let us denote by $\mathcal{P}_{e,SW}$ the probability of failure of the Slepian-Wolf decoder. According to Proposition 1 we obtain that, for $i = 1, 2, 3$,

$$\begin{aligned}D(Q_c, X_i^n) &\leq d_{c,i}(\mathcal{L}^{(n,r_0)}) \\ &\leq (\mathcal{P}_{X_1X_2X_3}(r_0) + \mathcal{P}_{e,SW})\Delta_{i,sup}^2 \\ &\quad + D(Q_c, X_i^n).\end{aligned} \tag{93}$$

According to [1], the value of $\mathcal{P}_{e,SW}$ can be decreased arbitrarily by enlarging the block size used by the Slepian-Wolf encoder. Leveraging the fact that $\Delta_{i,sup}$ is bounded, we conclude that the effect on the distortion of the Slepian-Wolf decoding failure can also be diminished arbitrarily. Combining this observation with (93) and with Lemma 4, it follows that, as the block size of the Slepian-Wolf coder goes to ∞, the following holds

$$\begin{aligned}D(Q_c, X_i^n) &\leq d_{c,i}(\mathcal{L}^{(n,r_0)}) \\ &\leq \mathcal{P}_{X_1X_2X_3}(r_0)\kappa_1^2 c_0^2 \nu_s^{\frac{2}{n}} + D(Q_c, X_i^n).\end{aligned} \tag{94}$$

According to Lemma 1 in [49], one has $D(Q_c, X_i^n) = G_c\nu_c^{\frac{2}{n}}(1 + o(1))$ in the limit of (6). Plugging this result in (94) leads to (8).

C. Proof of Relations (9)

Let us first denote $\bar{\mathcal{P}}_i \triangleq \mathbb{P}[Q_{in}(Q_c(X_i^n)) \in \mathcal{W}]$ and $\hat{\mathcal{P}}_i \triangleq \mathbb{P}[Q_{in}(Q_c(X_i^n)) \in \mathcal{S} | Q_{in}(Q_c(X_i^n)) \in \mathcal{W}]$, where $\mathcal{W}$ and $\mathcal{S}$ are defined in Section V-B. Additionally, for $0 \leq z \leq 1$, let $H_b(z) \triangleq -z\log_2 z - (1-z)\log_2(1-z)$. Further, note that the rate needed to transmit $\beta_i(\lambda_i)$ is $\frac{1}{n}H(Q_{\mathcal{A}_i}(X_i^n))$. The rate needed for a_i is $\frac{1}{n}H_b(\bar{\mathcal{P}}_i)$, while the rate for encoding $\hat{\lambda}_{f_i}$ equals $\frac{1}{n}\bar{\mathcal{P}}_i \log_2|\mathcal{L}| = \bar{\mathcal{P}}_i\log_2 c_0$. Since b_i is transmitted only when $a_i = 1$, the rate needed for b_i is $\frac{1}{n}\bar{\mathcal{P}}_i H_b(\hat{\mathcal{P}}_i)$. The rate used for encoding τ_i equals $\frac{1}{n}\bar{\mathcal{P}}_i\hat{\mathcal{P}}_i\log_2|\mathcal{T}| = \bar{\mathcal{P}}_i\hat{\mathcal{P}}_i\log_2 3$. Finally, the rate used for encoding u_1,u_2 and u_3 with a Slepian-Wolf coder, i.e., $\frac{1}{n}H(U_1, U_2, U_3)$, is equally divided among the three encoders. It follows that

$$\begin{aligned}R_i(\mathcal{L}^{(n,r_0)}) = \frac{1}{n}\Big(&H(Q_{\mathcal{A}_i}(X_i^n)) + \frac{1}{3}H(U_1, U_2, U_3) + H_b(\bar{\mathcal{P}}_i) \\ &+ \bar{\mathcal{P}}_i H_b(\hat{\mathcal{P}}_i)\Big) + \bar{\mathcal{P}}_i(\log_2 c_0 + \hat{\mathcal{P}}_i\log_2 3).\end{aligned} \tag{95}$$

Since $\lim_{(6)} \bar{r}(\mathcal{A}_i(\mathbf{0})) = 0$, as proved in Part 1 of the proof of relation (7), we can use Lemma 2 from [49] (proved by Csiszar in [51]) and the fact that $\nu(\mathcal{A}_i(\mathbf{0})) = \nu_s$ to obtain that

$$\lim_{(6)} \frac{1}{n} \left(H(Q_{\mathcal{A}_i}(X_i^n)) + \log_2(\nu_s) \right) = h(X_i). \tag{96}$$

Lemma 5, proved next, states that $\lim_{(6)}(\bar{\mathcal{P}}_i \log_2 c_0) = 0$. This implies that $\lim_{(6)} \bar{\mathcal{P}}_i = 0 = \lim_{(6)} \hat{\mathcal{P}}_i$ and further that $\lim_{(6)} H_b(\bar{\mathcal{P}}_i) = 0 = \lim_{(6)} H_b(\hat{\mathcal{P}}_i)$. The above considerations, together with equalities (95) and (96), imply relations (9).

Lemma 5. *For $i = 1, 2, 3$, one has $\lim_{(6)}(\bar{\mathcal{P}}_i \log_2 c_0) = 0$.*

Proof: Let us fix i. Denote

$$\tilde{\mathcal{W}}(\lambda_f) \triangleq \{x_i^n \in \mathbb{R}^n : Q_{in}(Q_c(x_i^n)) \in \mathcal{W}(\lambda_f)\}$$

and $\tilde{\mathcal{W}} \triangleq \cup_{\lambda_f \in \Lambda_f} \tilde{\mathcal{W}}(\lambda_f)$. Thus, $\bar{\mathcal{P}}_i = \mathbb{P}[X_i^n \in \tilde{\mathcal{W}}]$. A moment of thought reveals that

$$\tilde{\mathcal{W}}(\lambda_f) \subset (\lambda_f + \eta_1 V_f(\mathbf{0})) \setminus (\lambda_f + \eta_2 V_f(\mathbf{0})),$$

where $\eta_1 \triangleq 1 + \frac{\bar{r}_{in} + \bar{r}_c}{r_f}$ and $\eta_2 \triangleq \eta - \frac{\bar{r}_{in} + \bar{r}_c}{r_f} = 1 - \frac{4\bar{r}_{in} + \bar{r}_c}{r_f}$. The above relation implies that

$$\nu(\tilde{\mathcal{W}}(\lambda_f)) \leq (\eta_1^n - \eta_2^n)\nu_f. \tag{97}$$

Since f_{X_i} has finite variance, it follows that $\mathbb{E}[\|X_i^n\|] \in \mathbb{R}$. Let $\rho_1(c_0) \triangleq \mathbb{E}[\|X_i^n\|](\log_2 c_0)^2$. Markov's inequality implies that $\mathbb{P}[\|X_i^n\| \geq \rho_1(c_0)] \leq \frac{1}{(\log_2 c_0)^2}$. It follows that

$$\bar{\mathcal{P}}_i \leq \underbrace{\mathbb{P}[X_i^n \in \tilde{\mathcal{W}} \cap \mathcal{B}_{\rho_1(c_0)}]}_{T_1} + \underbrace{\mathbb{P}[X_i^n \notin \mathcal{B}_{\rho_1(c_0)}]}_{T_2}.$$

Since $T_2 \leq \frac{1}{(\log_2 c_0)^2}$, in order to prove the lemma it is sufficient to show that $\lim_{(6)}(T_1 \log_2 c_0) = 0$. For this, let us denote $B_0 \triangleq \sup\{f_{X_i}(x^n) | x^n \in \mathbb{R}^n)\}$, which is finite since f_{X_i} is bounded. Note that if $x_i^n \in \mathcal{B}_{\rho_1(c_0)}$ then $Q_f(Q_{in}(Q_c(x_i^n))) \in \mathcal{B}_{\rho_2(c_0)}$, where $\rho_2(c_0) \triangleq \rho_1(c_0) + \bar{r}_c + \bar{r}_{in} + \bar{r}_f$. Then one has

$$\begin{aligned} T_1 &\leq \sum_{\lambda_f \in \Lambda_f \cap \mathcal{B}_{\rho_2(c_0)}} \int_{\tilde{\mathcal{W}}(\lambda_f)} f_{X_i^n}(x^n) dx^n \\ &\leq \sum_{\lambda_f \in \Lambda_f \cap \mathcal{B}_{\rho_2(c_0)}} B_0 \nu(\tilde{\mathcal{W}}(\lambda_f)) \\ &\overset{(a)}{\leq} B_0(\eta_1^n - \eta_2^n) \sum_{\lambda_f \in \Lambda_f \cap \mathcal{B}_{\rho_2(c_0)}} \nu_f \\ &\overset{(b)}{\leq} B_0(\eta_1^n - \eta_2^n)\nu(\mathcal{B}_{\rho_2(c_0)+\bar{r}_f}), \end{aligned} \tag{98}$$

where (a) is obtained using (97), while (b) holds since $\cup_{\lambda_f \in \Lambda_f \cap \mathcal{B}_{\rho_2(c_0)}} V_f(\lambda_f) \subseteq \mathcal{B}_{\rho_2(c_0)+\bar{r}_f}$. Further,

$$\begin{aligned} (\eta_1^n - \eta_2^n) &= (\eta_1 - \eta_2)(\eta_1^{n-1} + \eta_1^{n-2}\eta_2 + \eta_1^{n-3}\eta_2^2 + \cdots + \eta_2^{n-1}) \\ &\leq (\eta_1 - \eta_2) n \eta_1^{n-1}. \end{aligned} \tag{99}$$

Relations (98) and (99), together with $\lim_{(6)} \eta_1 = 1$ and $\nu(\mathcal{B}_{\rho_2(c_0)+\bar{r}_f}) = \nu(\mathcal{B}_1)(\rho_2(c_0) + \bar{r}_f)^n$, imply that, in order to conclude the proof, it is enough to prove that

$$\lim_{(6)}((\eta_1 - \eta_2)(\rho_2(c_0) + \bar{r}_f)^n \log_2 c_0) = 0. \tag{100}$$

Let $\bar{r} \triangleq \bar{r}_c + \bar{r}_{in} + 2\bar{r}_f$. Then

$$\begin{aligned} &(\eta_1 - \eta_2)(\rho_2(c_0) + \bar{r}_f)^n \log_2 c_0 \\ &= \frac{5\theta\bar{r}_{in,0} + 2\theta\bar{r}_{c,0}}{c_0\theta r_{in,0}} \left(\mathbb{E}[\|X_i^n\|](\log_2 c_0)^2 + \bar{r} \right)^n \log_2 c_0 \\ &= \frac{5\bar{r}_{in,0} + 2\bar{r}_{c,0}}{r_{in,0}} \left(\mathbb{E}[\|X_i^n\|] \frac{(\log_2 c_0)^{2+\frac{1}{n}}}{c_0^{\frac{1}{n}}} + \bar{r}\left(\frac{\log_2 c_0}{c_0}\right)^{\frac{1}{n}} \right)^n. \end{aligned}$$

Using further the relations $\lim_{(6)} \bar{r} = 0$, $\lim_{(6)} (\frac{\log_2 c_0}{c_0})^{\frac{1}{n}} = 0$ and $\lim_{(6)} \frac{(\log_2 c_0)^{2+\frac{1}{n}}}{c_0^{\frac{1}{n}}} = 0$, (100) follows. This completes the proof of Lemma 5. ■

ACKNOWLEDGMENT

The authors would like to thank the Editor and the anonymous reviewers for their valuable comments and suggestions, which helped improve the quality of the work.

REFERENCES

[1] D. Slepian and J. K. Wolf, "Noiseless coding of correlated information sources," *IEEE Trans. Inform. Theory*, vol. IT-19, no. 4, pp. 471–480, Jul. 1973.

[2] A. D. Wyner and J. Ziv, "The rate-distortion function for source coding with side information at the decoder," *IEEE Trans. Inform. Theory*, vol. IT-22, no.1, pp. 1–10, Jan. 1976.

[3] T. Berger, "Multiterminal source coding," in *The Information Theory Approach to Communications (CISM Courses and Lectures, no. 229)*, G. Longo, Ed. Vienna/New York: Springler-Verlag, 1978, pp. 171–231.

[4] S. Y. Tung, "Multiterminal Source Coding," Ph.D. dissertation, School of Electrical Engineering, Cornell Univ. Ithaca, NY, May 1978.

[5] T. Berger and R. W, Yeung, "Multiterminal source encoding with one distortion criterion," *IEEE Trans. Inform. Theory*, vol. 35, no. 2, pp. 228–236, Mar. 1989.

[6] Y. Oohama, "Gaussian multiterminal source coding," *IEEE Trans. Inf. Theory*, vol. 43 no. 6, pp. 1912–1923, Nov. 1997.

[7] A. B. Wagner, S. Tavildar, and P. Viswanath, "Rate region of the quadratic Gaussian two-encoder source-coding problem," *IEEE Trans. Inform. Theory*, vol. 54, no. 5, pp. 1938–1961, May 2008.

[8] J. Wang, J. Chen, and X. Wu, "On the sum rate of Gaussian multiterminal source coding: New proofs and results," *IEEE Trans. Inform. Theory*, vol. 56, no. 8, pp. 3946–3960, Aug. 2010.

[9] J. Wang and J. Chen, "Vector Gaussian two-terminal source coding," *IEEE Trans. Inform. Theory*, vol. 59, no. 6, pp. 3693–3708, Jun. 2013.

[10] J. Wang and J. Chen, "Vector Gaussian multiterminal source coding," *IEEE Trans. Inform. Theory*, vol. 60, no. 9, pp. 5533–5552, Sept. 2014.

[11] T. Berger, Z. Zhang, and H. Viswanathan, "The CEO problem [multiterminal source coding]," *IEEE Trans. Inform. Theory*, vol. 42, no. 3, pp. 887–902, May 1996.

[12] Y. Oohama, "Rate-distortion theory for Gaussian multiterminal source coding systems with several side informations at the decoder," *IEEE Trans. Inform. Theory*, vol. 51, no. 7, pp. 2577–2593, Jul. 2005.

[13] V. Prabhakaran, D. N. C. Tse, and K. Ramchandran, "Rate region of the quadratic Gaussian CEO problem," in *Proc. IEEE Intern. Symp. Inform. Theory*, Chicago, IL, Jun./Jul. 2004, p. 119.

[14] P. Ishwar, R. Puri, K. Ramchandran, and S. S. Pradhan, "On rate-constrained distributed estimation in unreliable sensor networks," *IEEE J. Selec. Areas Commun.*, vol. 23, no. 4, pp. 765–775, Apr. 2005.

[15] J. Chen and T. Berger, "Robust distributed source coding," *IEEE Trans. Inform. Theory*, vol. 54, no. 8, pp. 3385–3398, Aug. 2008.

[16] A. Saxena, J. Nayak, and K. Rose, "On efficient quantizer design for robust distributed source coding," in *Proc. IEEE Data Compress. Conf.*, Snowbird, UT, Mar. 2006, pp. 63–72.

[17] A. Saxena and K. Rose, "On scalable distributed coding of correlated sources," *IEEE Trans. Signal. Proc.*, vol. 58, no. 5, pp. 2875–2883, May 2010.

[18] X. Wu, A. Bais, and N. Sarshar, "Quantization for robust distributed coding," *Intern. J. Distributed Sensor Networks*, vol. 2016, pp. 1–6, May 2016.

[19] R. Zamir, S. Shamai, and U. Erez, "Nested linear/lattice codes for structured multiterminal binning," *IEEE Trans. Inform. Theory*, vol. 48, no. 6, pp. 1250–1276, Jun. 2002.

[20] S. D. Servetto, "Lattice quantization with side information: codes, asymptotics, and applications in sensor networks," *IEEE Trans. Inform. Theory*, vol. 53, no. 2, pp. 714–731, Feb. 2007.

[21] D. Krithivasan and S. S. Pradhan, "Lattices for distributed source coding: Jointly Gaussian sources and reconstruction of a linear function," *IEEE Trans. Inform. Theory*, vol. 55, no. 12, pp. 5628–5651, Dec. 2009.

[22] A. Reani and N. Merhav, "Universal quantization for separate encodings and joint decoding of correlated sources," *IEEE Trans. Inform. Theory*, vol. 61, no. 12, pp. 6465–6474, Dec. 2015.

[23] L. Ozarow, "On a source coding problem with two channels and three receivers," *Bell Syst. Tech. J.*, vol. 59, no.10, pp. 1909–1921, Dec. 1980.

[24] A. A. El Gamal and T. M. Cover, "Achievable rates for multiple descriptions," *IEEE Trans. Inform. Theory*, vol. IT-28, no. 6, pp. 851–857, Nov. 1982.

[25] R. Venkataramani, G. Kramer, and V. K. Goyal, "Multiple description coding with many channels," *IEEE Trans. Inform. Theory*, vol. 49, no. 9, pp. 2106–2114, Sep. 2003.

[26] H. Wang and P. Viswanath, "Vector Gaussian multiple description with two levels of receivers," *IEEE Trans. Inform. Theory*, vol. 55, no. 1, pp. 401–410, Jan. 2009.

[27] J. Chen, "Rate region of Gaussian multiple description coding with individual and central distortion constraints," *IEEE Trans. Inform. Theory*, vol. 55, no. 9, pp. 3991–4005, Sept. 2009.

[28] J. Wang, J. Chen, L. Zhao, P. Cuff, and H. Permuter, "On the role of the refinement layer in multiple description coding and scalable coding," *IEEE Trans. Inform. Theory*, vol. 57, no. 3, pp. 1443–1456, Mar. 2011.

[29] Y. Zhang, S. Dumitrescu, J. Chen, Z. Sun, "LDGM-based multiple description coding for finite alphabet sources," *IEEE Trans. Communications*, vol. 60, no. 12, pp. 3671-3682, Dec. 2012.

[30] L. Song, S. Shuo, and J. Chen, "A lower bound on the sum rate of multiple description coding with symmetric distortion constraints," *IEEE Trans. Inform. Theory*, vol. 60, no. 12, pp. 7547–7567, Dec. 2014.

[31] H. Wu, T. Zheng, and S. Dumitrescu, "On the design of symmetric entropy-constrained multiple description scalar quantizer with linear joint decoders," *IEEE Trans. Communications*, vol. 65, no. 8, pp. 3453–3466, Aug. 2017.

[32] V. A. Vaishampayan, N. Sloane, and S. Servetto, "Multiple description vector quantization with lattice codebooks: design and analysis," *IEEE Trans. Inform. Theory*, vol. 47, no. 5, pp. 1718–1734, Jul. 2001.

[33] S. N. Diggavi, N. Sloane, and V. A. Vaishampayan, "Asymmetric multiple description lattice vector quantizers," *IEEE Trans. Inform. Theory*, vol. 48, no. 1, pp. 174–191, Jan. 2002.

[34] V. K. Goyal, J. A. Kelner, and J. Kovacevic, "Multiple description vector quantization with a coarse lattice," *IEEE Trans. Inform. Theory*, vol. 48, no. 3, pp. 781–788, Mar. 2002.

[35] X. Huang and X. Wu, "Optimal index assignment for multiple description lattice vector quantization," *Data Compression Conf.*, pp. 272–281, Snowbird, UT, Mar. 2006.

[36] J. Ostergaard, J. Jensen, and R. Heusdens, "n-channel entropy-constrained multiple description lattice vector quantization," *IEEE Trans. Inform. Theory*, vol. 52, no. 5, pp. 1956–1973, May 2006.

[37] J. Chen, C. Tian, T. Berger, and S. S. Hemami, "Multiple description quantization via Gram-Schmidt orthogonalization," *IEEE Trans. Inform. Theory*, vol. 52, no. 12, pp. 5197-5217, Dec. 2006.

[38] M. Liu and C. Zhu, "M-description lattice vector quantization: index assignment and analysis," *IEEE Trans. Signal Proc.*, vol. 57, no. 6, pp. 2258–2274, Jun. 2009.

[39] J. Ostergaard and R. Zamir, "Multiple-description coding by dithered delta-sigma quantization," *IEEE Trans. Inform. Theory*, vol. 55, no. 10, pp. 4661-4675, Oct. 2009.

[40] J. Ostergaard, R. Heusdens, and J. Jensen, "n-channel asymmetric entropy-constrained multiple-description lattice vector quantization," *IEEE Trans. Inform. Theory*, vol. 56, no. 12, pp. 6354–6375, Dec. 2010.

[41] G. Zhang, J. Ostergaard, J. Klejsa, and W. B. Kleijn, "High-rate analysis of symmetric L-channel multiple description coding," *IEEE Trans. Commun.*, vol. 59, no. 7, pp. 1846–1856, Jul. 2011.

[42] Z. Gao and S. Dumitrescu, "Flexible symmetric multiple description lattice vector quantizer with $L \geq 3$ descriptions," *IEEE Trans. Commun.*, vol. 62, no. 12, pp. 4281–4292, Dec. 2014.

[43] S. Dumitrescu, Y. Chen, and J. Chen, "Index mapping for bit-error resilient multiple description lattice vector quantizer," *IEEE Trans. Commun.*, vol. 66, no. 8, pp. 3638–3652, Aug. 2018.

[44] D. Elzouki, S. Dumitrescu and J. Chen, "Lattice-based robust distributed source coding," *IEEE Trans. Inform. Theory*, vol. 65, no. 3, pp. 1764–78, Mar. 2019.

[45] D. Elzouki, S. Dumitrescu, and J. Chen, "Lattice-based robust distributed source coding for three correlated sources," *Proc. 16th Canadian Workshop Inform. Theory*, Hamilton, Canada, June 2-5, 2019.

[46] R. Zamir, *Lattice coding for signals and networks*, Cambridge University Press, 2014.

[47] R. Zamir and M. Feder, "On lattice quantization noise, "*IEEE Trans. Inf. Theory*, vol. 42, no. 4, pp. 1152–1159, Jul. 1996.

[48] J. H. Conway and N. J. A. Sloane, *Sphere packings, lattices and groups*, 3rd Ed., Springer, New York, 1999.

[49] T. Linder and K. Zeger, "Asymptotic entropy-constrained performance of tessellating and universal randomized lattice quantization," *IEEE Trans. Inform. Theory*, vol. 40, no. 2, pp. 575–579, Mar. 1994.

[50] H. Scheffe, "A useful convergence theorem for probability distributions," *Ann. Math. Statist.*, vol. 18, no. 3, pp. 434–438, Sept. 1947.

[51] I. Csiszar, "Generalized entropy and quantization problems," in *Trans. Sixth Prague Conf. Inform. Theory, Statis. Decision Functions, Random Processes*, Prague, pp. 29–35, Akademia, 1973.

Sorina Dumitrescu (M'05-SM'13) received the B.Sc. and Ph.D. degrees in mathematics from the University of Bucharest, Romania, in 1990 and 1997, respectively. From 2000 to 2002 she was a Postdoctoral Fellow in the Department of Computer Science at the University of Western Ontario, London, Canada. Since 2002 she has been with the Department of Electrical and Computer Engineering at McMaster University, Hamilton, Canada, where she held a Postdoctoral and a Research Associate position, and where she is currently an Associate Professor. Her current research interests include theoretical and practical aspects of source coding and joint source-channel coding. Her earlier research interests were in formal languages and automata theory. She was a recipient of the NSERC University Faculty Award during 2007-2012.

Dania Elzouki received the B.Sc. degree in electrical and electronic engineering from the University of Benghazi (formerly known as Garyounis University), Libya, in 2005. She received the M.Eng. and Ph.D. degrees in electrical and computer engineering from McMaster University, Hamilton, ON, Canada in 2013 and 2018, respectively. Her research interests include wireless communications, signal processing and information theory.

Jun Chen (Senior Member, IEEE) received the B.E. degree in communication engineering from Shanghai Jiao Tong University, Shanghai, China, in 2001 and the M.S. and Ph.D. degrees in electrical and computer engineering from Cornell University, Ithaca, NY, USA, in 2004 and 2006, respectively.

He was a Postdoctoral Research Associate with the Coordinated Science Laboratory, University of Illinois at Urbana-Champaign, Urbana, IL, USA, from September 2005 to July 2006, and a Postdoctoral Fellow at the IBM Thomas J. Watson Research Center, Yorktown Heights, NY, USA, from July 2006 to August 2007. Since September 2007, he has been with the Department of Electrical and Computer Engineering, McMaster University, Hamilton, ON, Canada, where he is currently a Professor. His research interests include information theory, machine learning, wireless communications, and signal processing.

Dr. Chen was a recipient of the Josef Raviv Memorial Postdoctoral Fellowship in 2006, the Early Researcher Award from the Province of Ontario in 2010, the IBM Faculty Award in 2010, and the JSPS Invitational Fellowship in 2020. He held the title of the Barber-Gennum Chair in Information Technology from 2008 to 2013 and the Joseph Ip Distinguished Engineering Fellow from 2016 to 2018. He served as an Associate Editor of the IEEE Transactions on Information Theory from 2014 to 2016. He is currently an Editor of the IEEE Transactions on Green Communications and Networking.